AD 423420

UNIVERSITY OF NEW MEXICO

ALBUQUERQUE

ENGINEERING EXPERIMENT STATION

TECHNICAL REPORT EE-100

INPUT IMPEDANCE AND RADIATION EFFICIENCY CHARACTERISTICS OF VLF TRAILING-WIRE ANTENNAS AND VLF SIDE-LOADED TRANSMISSION-LINE ANTENNAS

by

H. D. WADE

OCTOBER, 1963

This work was performed under Contract Nonr 2798(00) (NR-)

INPUT IMPEDANCE AND RADIATION EFFICIENCY CHARACTERISTICS OF VLF TRAILING-WIRE ANTENNAS AND VLF SIDE-LOADED TRANSMISSION-LINE ANTENNAS

EE-100

by

H. D. Wade

The University of New Mexico
Albuquerque, New Mexico
October, 1963

This work was performed under
Contract Nonr 2798(01)(FBM)

ABSTRACT

This report presents a comparison in free space of input impedance and radiation efficiency characteristics of two types of radiating structures which have been proposed for use as airborne VLF antennas: namely, the single "trailing-wire antenna" and the side-loaded "transmission-line antenna."

A mathematical model for a trailing-wire antenna, based on equations derived by S. A. Schelkunoff for the input impedance of long cylindrical wires, is used for the calculation of the input impedance of trailing-wire antennas. Experimental measurements are presented in support of this model. Theoretical calculations of input impedance and radiation efficiency are given for three "typical" VLF trailing-wire antennas. The input impedance is strongly dependent upon the static capacitance of the aircraft. Efficiencies of 70% to 90% can be obtained for copper wires with lengths near $\lambda/2$; while 5% to 15% is typical for very short electrical lengths.

From the theory of side-loaded transmission-line antennas derived by R. W. Kulterman, input impedance, radiation efficiency, and side-load voltage drops are calculated for examples of three types of transmission-line antennas. Some general comparisons are made between the efficiency and impedance characteristics of trailing-wire antennas and transmission-line antennas. Some advantages and disadvantages of both types of antennas are given.

TABLE OF CONTENTS

ACKNOWLEDGEMENTS

The author expresses his appreciation to Professors R. H. Williams, R. D. Kelly, and J. S. Lambert for their advice in the performance of this investigation, and to the United States Navy, which sponsored the research needed for the preparation of this report.

The author gratefully acknowledges the cooperation of the Boeing Airplane Company in permitting the use of experimental data taken from an unpublished internal company report on trailing-wire antennas. Without the use of this data, it is doubtful that this report could have been written.

Appreciation is also expressed to H. B. Orton, R. A. Young, and L. R. Rice for their programming and running of the computer calculations.

The author is very appreciative of the conscientious work of the typist, Miss Jane Anderson, and of the draftsman, Mr. Terry Anna.

LIST OF FIGURES

LIST OF FIGURES (Cont'd)

LIST OF FIGURES (Cont'd)

1.0 INTRODUCTION

In recent years a need has arisen for the development of airborne transmitting stations capable of radiating large amounts of power as efficiently as possible in the VLF spectrum. This report is concerned with two types of antennas which have been proposed for use as airborne VLF antennas; specifically: (1) a single long wire (either bare or insulated), trailing behind an aircraft equipped with a transmitter, and driven with respect to the aircraft; henceforth this antenna will be designated "the trailing-wire antenna." (2) A linear side-loaded transmission-line antenna trailing behind an aircraft and driven from an airborne transmitter with the aircraft forming only a passive part of the radiating structure; henceforth this antenna will be designated "the transmission-line antenna." Both types are shown schematically in Figure 1.

The scope of this report is primarily limited to the electrical properties of these two antennas; however, a few general comments on some mechanical and aerodynamical aspects will be included. The major portion of this report is concerned with the development and justification of a suitable mathematical model and theory by means of which the input impedance and radiation efficiency of a VLF-LF trailing-wire antenna may be calculated. Experimental measurements performed independently of this investigation are reported in support of the theory [1].

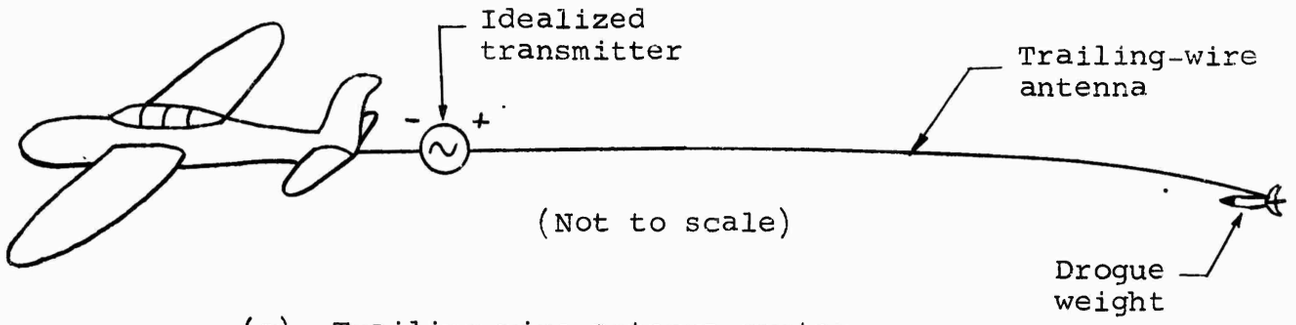

(a) Trailing-wire antenna system

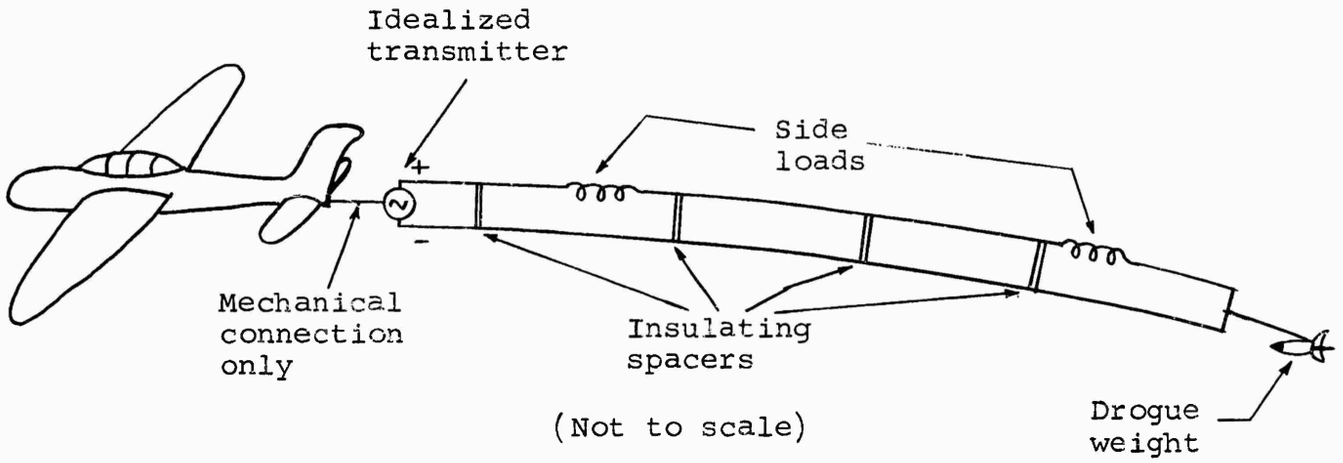

(b) Side-loaded transmission-line antenna system

Figure 1. Airborne trailing-wire and side-loaded transmission-line antenna systems

Theoretical calculations of the input impedance and radiation efficiency are presented for trailing-wire antennas with 0.10-inch diameter and lengths of 10,000, 15,000, and 25,000 feet, respectively.

A comprehensive theory of the input impedance and radiation efficiency of electrically short side-loaded transmission-line antennas has been previously developed by R. W. Kulterman [2], and will not be given in detail in this report; however, the results of this theory are used to calculate input impedance, radiation efficiency and side-load voltage drops of selected VLF transmission-line antennas. The characteristics of these transmission-line antennas are then compared with those of the trailing-wire antennas, and conclusions drawn from the comparison are presented.

2.0 INPUT IMPEDANCE OF VLF TRAILING-WIRE ANTENNAS

2.1 Theoretical Considerations

For operation in air in the VLF spectrum, any linear antenna must be physically long if it is to have any appreciable electrical length. For example, an antenna operating in air at 30 kc (upper limit of VLF spectrum), and having an electrical length of one-half wavelength, would have to be 16,400 feet long. Clearly, at the lower VLF frequencies any practical trailing-wire antenna will be electrically fairly short. The towing aircraft will be so short at VLF wavelengths that it will give a negligible contribution to the radiation field (far-zone field) of the antenna. The towing aircraft does, however, have an appreciable effect on the input impedance of a trailing-wire antenna, and cannot be neglected in any realistic mathematical model.

Since the towing aircraft is very small with respect to VLF wavelengths, it is not realistic to consider the trailing-wire antenna as a thin monopole above a ground plane, even as a first approximation. The trailing-wire antenna might be considered as an asymmetrically-driven cylindrical antenna having arms with different effective radii. King [3] has presented a simple method for calculating the input impedance of electrically short, thin asymmetrical cylindrical antennas; however, it is believed that this method is not valid for the

extremes of asymmetry presented by the trailing-wire antenna. Schelkunoff [4] has postulated that the idealized structure shown in Figure 2c represents all the essential features of the end-fed antenna of Figure 2a, which consists of a generator with one terminal left floating and the other terminal connected to a long wire. The antenna is effectively driven against the capacitance of the generator. The impedance of the antenna shown in Figure 2c as seen at point P equals the impedance of the antenna proper (the cone) in series with the capacitive impedance of the sphere. There is also a parallel capacitance shunting the cone and the sphere. The capacitance of the small sphere of radius b in series with the cone is given by

$$C_{sphere} = \frac{4\pi\epsilon b}{1 - \frac{1}{2}\ln\left(\frac{2}{\Psi}\right)}, \qquad (1)$$

where ϵ is the dielectric permittivity of the surrounding medium, and Ψ is the half angle of the cone. The numerator of (1) is the capacitance of the sphere in free space, while the denominator expresses the effect of the cone. If δ and Ψ are both small (See Fig. 2c), and yet δ is large compared with Ψ, then the capacitance shunting the cone and the sphere is given by

$$C_{shunt} = \frac{\pi\epsilon b\left(1 + \frac{\pi^2}{6}\right)}{\left[\ln\left(\frac{2}{\Psi}\right)\right]^2}. \qquad (2)$$

The impedance, Z_c, of a thin cone of length ℓ is given by

$$Z_c = K\,\frac{Z_a \sin(\beta\ell) - j(K + 60)\cos(\beta\ell)}{(K + 60)\sin(\beta\ell) - jZ_a\cos(\beta\ell)} \qquad (3a)$$

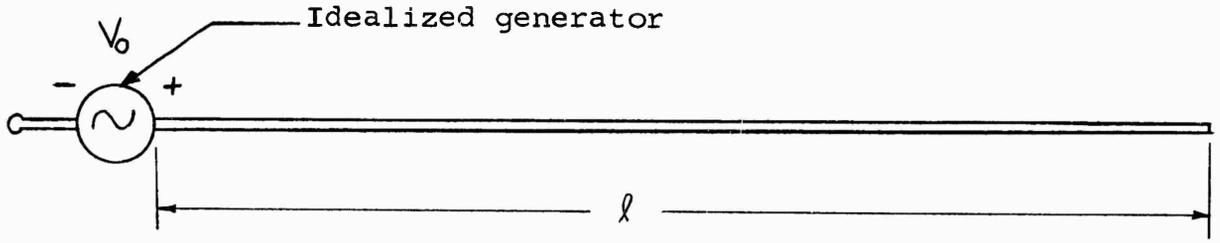

(a) Long wire driven against generator capacitance

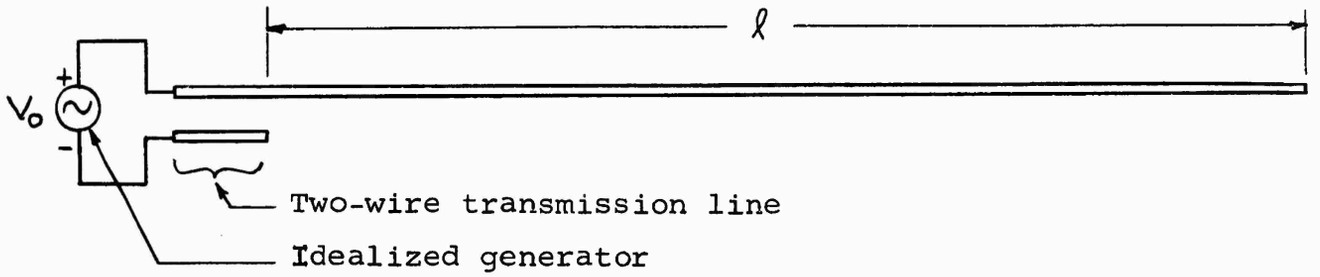

(b) A practical method of end-feeding a long wire

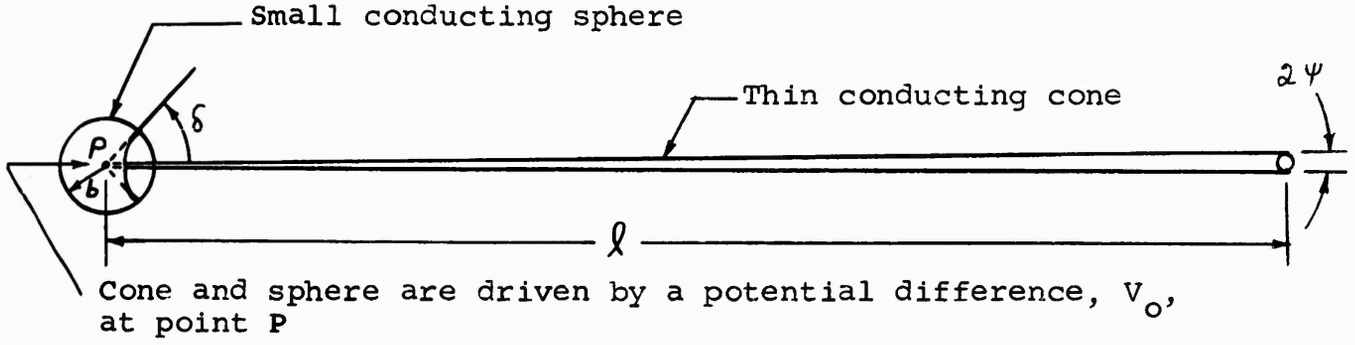

(c) Idealized model for an end-fed antenna

Figure 2. Theoretical models of a VLF trailing-wire antenna

where

$$K = 60 \ln\left(\frac{2}{\Psi}\right) - 30, \tag{3b}$$

$$Z_a = R_a + jX_a = 30\,\mathrm{Ein}(2\beta\ell) - 15(1 - e^{-j2\beta\ell}), \tag{3c}$$

and

$$\beta = \frac{2\pi}{\lambda} \tag{3d}$$

Equations (1) through (3c) are taken directly from [4, p. 80].

Equations (1) and (2) are of practical interest only insofar as they illustrate the general effects of the driving-point region on the input impedance. For a practical trailing-wire antenna, the aircraft and the wire will not likely be closely coupled, i. e., $\delta >> \Psi$ and $C_{shunt} << C_{sphere}$, and the effects of the shunt capacitance may be neglected to a first-order approximation. The actual value of the series capacitance of the aircraft (represented by the sphere) would have to be determined empirically in each specific case. As a first approximation to the input impedance of a thin cylindrical wire of length ℓ, the input impedance of a thin cone of length ℓ, given by (3a), might be used. Such an approximation is not very satisfactory because uncertainty exists concerning the proper value of Ψ to be used in (3b). Equation (3a) was originally derived by Schelkunoff as a result of his rigorous classical solution of the thin, center-fed biconical antenna. The geometry of the cylindrical wire does not readily lend itself to direct solution as a boundary value problem; however, Schelkunoff has given a method for obtaining a second-order approximation to the input impedance of a thin linear antenna of any cross-section by means of wave perturbation

techniques [5]. Application of the wave perturbation technique to a thin dipole antenna gives three important parameters [6]:

$$K[z,\ \rho(z)] = 120 \ln\left[\frac{2z}{\rho(z)}\right] \tag{4}$$

$$M(\beta\ell) = \beta\int_0^{\ell}[K_a - K(z,\rho)]\sin(2\beta z)\,dz \quad , \tag{5}$$

and

$$N(\beta\ell) = \beta\int_0^{\ell}[K_a - K(z,\rho)]\cos(2\beta z)\,dz \quad , \tag{6}$$

where $K[z,\rho(z)]$ is the nominal characteristic impedance of the antenna in air at any distance z from the driving point, $\rho(z)$ is the radius of the antenna at a distance z from the driving point, and K_a is the average of $K[z,\rho(z)]$ over the entire length of the antenna. The quantities $M(\beta\ell)$ and $N(\beta\ell)$ express the effects of the departure of $K[z,\rho(z)]$ from K_a. For a cylindrical antenna, $\rho(z) = a$ (a = wire radius), and it may be verified from (4), (5) and (6) that for a cylindrical antenna,

$$M(\beta\ell) = 60[\mathrm{Cin}\ (2\beta\ell) - 1 + \cos\ (2\beta\ell)] \tag{7}$$

$$N(\beta\ell) = 60[\mathrm{Si}\ (2\beta\ell) - \sin\ (2\beta\ell)] \tag{8}$$

$$K_a = 120[\ln(\tfrac{2\ell}{a}) - 1]. \tag{9}$$

Schelkunoff has included the effects expressed by (4), (5), and (6) into an expression which gives the input impedance in air of an end-fed antenna of any shape,[1]

$$Z = K_a\,\frac{R_a\sin(\beta\ell) + j\{[X_a - N(\beta\ell)]\sin(\beta\ell) - [K_a + 60 - M(\beta\ell)]\cos(\beta\ell)\}}{\{[K_a + 60 + M(\beta\ell)]\sin(\beta\ell) + [X_a + N(\beta\ell)]\cos(\beta\ell)\} - jR_a\cos(\beta\ell)} \tag{10}$$

[1] See reference [4], p. 81, equation (236).

To apply (10) to an end-fed trailing-wire antenna, it is necessary to use one-half the values of $M(\beta\ell)$, $N(\beta\ell)$, and K_a as given in (7), (8), and (9). The quantities R_a and X_a are tabulated as functions of ℓ/λ in [4, p. 195] or they can be computed by

$$R_a(\beta\ell) = 30[\text{Cin}\,(2\beta\ell) - \sin^2(\beta\ell)] \qquad (11)$$

$$X_a(\beta\ell) = 30\ \text{Si}\,(2\beta\ell) - 15\sin(2\beta\ell)\ . \qquad (12)$$

The quantities $M(\beta\ell)$ and $N(\beta\ell)$ as given by (7) and (8) are also tabulated as functions of ℓ/λ in [4, p. 204].

It is now assumed that the capacitive coupling between the towing aircraft and the trailing-wire antenna is small and that the input impedance of a trailing-wire antenna can be represented by the equivalent circuit shown in Figure 3.

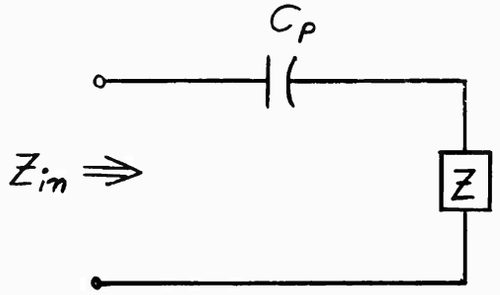

Figure 3. Equivalent circuit for input impedance of a trailing-wire antenna.

In Figure 3, C_p is an equivalent capacitance of the aircraft, which may be determined in some empirical manner from free-space capacitance and ground-plane capacitance measurements. One experimental method for determining C_p is given in [1, p. 35]. The impedance, Z, is computed from (10), with previously mentioned modifications.

Buehler and Lunden [1] have proposed an equivalent circuit similar to that of Figure 3, except that they couple the aircraft capacitance, C_p, to the wire impedance, Z, by means of an ideal transformer whose turns ratio is determined empirically. They found the transformer necessary to obtain agreement between theoretical and experimental input impedance values. Buehler and Lunden compute Z by taking one-half the values of Z for a center-fed dipole whose half-length is equal to the length of the wire. This effectively assumes that the trailing-wire acts as a monopole over an infinite conducting plane. It is believed that this assumption is not valid, and that the ideal transformer is unnecessary, provided that (10) is used to compute the impedance of the wire.

The reasoning leading to (10) and the equivalent circuit of Figure 3 has been largely heuristic in nature; no rigorous analysis has been presented. Before the experimental supporting data is presented in the next section, it is worthwhile to make a few general observations. Since the aircraft is extremely small compared to VLF wavelengths, it should have very little effect on the radiation (far-zone) fields of the antenna. As a result, the input resistance, which depends only on the far-zone fields in the ideal case, should be very nearly equal to the resistive part of the impedance as given by (10), if the wire is a good conductor. Since (10) was derived under the assumption of a perfectly conducting wire, it cannot be expected

to give accurate values of input resistance for wires of relatively poor conductivity. The input reactance of a trailing-wire antenna is largely determined by the configuration of the near-zone fields. The complex shape of the aircraft causes appreciable distortion of the fields near the aircraft; consequently the reactive part of the wire impedance as given by (10) will be less accurate than the resistive part. The input reactance as given by the equivalent circuit will also have some inaccuracy due to the indeterminacy in the proper value of C_p and the undetermined amount of capacitive coupling between the aircraft and the wire, which has been neglected.

2.2 Numerical Studies of Trailing-Wire Antennas

In order to support the validity of the equivalent circuit of Figure 3, some experimental measurements on trailing-wire antennas conducted by the Boeing Airplane Company [1] will be compared with the theoretical values given by the equivalent circuit. The experimental measurements were conducted in the LF-MF spectrum (150-1000 kc) using wires suspended vertically from a helicopter hovering above the sea. Even in this frequency range the assumption may be made that the helicopter has no significant electrical length. During these experiments the helicopter was hovering at an altitude sufficiently high to minimize the effects of reflections from the sea on the input impedance.

Figure 4 shows a comparison of the theoretical input resistance as computed by (10) with the measured input resistance of a Bell 47-G helicopter supporting a 580-ft. heavy litz wire with a diameter of 0.04 inches. This wire is a relatively good conductor, as the measured ohmic resistance is 0.025 Ω/ft at 680 kc. The agreement between theory and experiment is very good except near half-wave antiresonance ($0.45 < \ell/\lambda < 0.50$), where experimental values are somewhat lower than predicted by theory. The discrepancy near half-wave antiresonance is attributed to the effects of the ohmic losses in the wire.

A comparison of the theoretical and experimental input reactance of the antenna of Figure 4 is shown in Figure 5. The value of C_p for use in the equivalent circuit was taken to be the arithmetic mean of the helicopter capacitance measured in free space with respect to an infinite sphere enclosing the aircraft and the helicopter capacitance as measured with respect to a ground plane. For the Bell 47-G helicopter, C_p was found to be 280 pf. In Figure 5 the agreement between theory and experiment is generally not as good as that in Figure 4. The agreement could be improved somewhat by choosing C_p to be somewhat less than 280 pf; however, one has no a priori knowledge of the "best" value of C_p. The agreement is poorest near half-wave antiresonance, illustrating the effects of the ohmic losses in the wire.

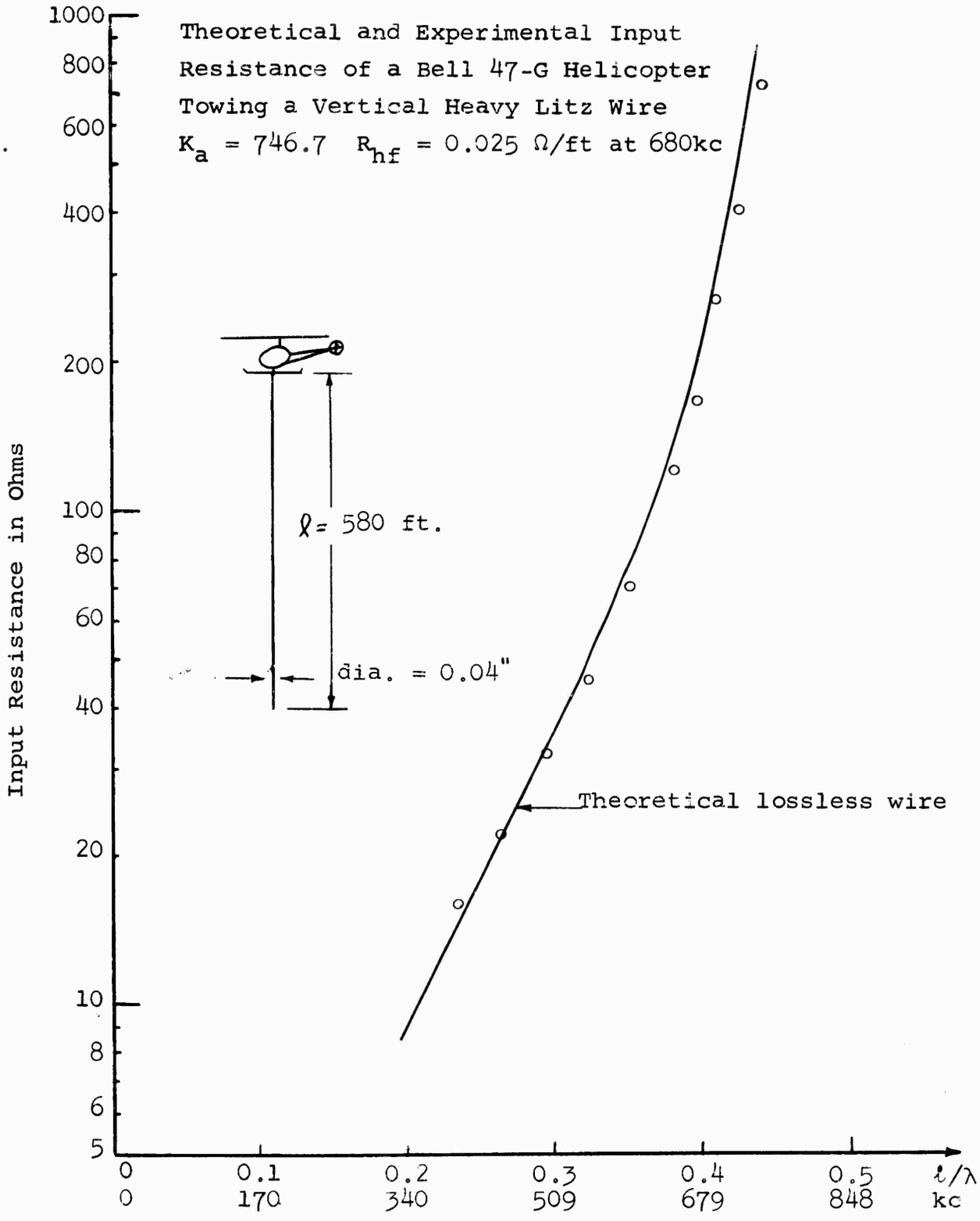

Figure 4. Theoretical and experimental input resistance of a 580-ft. trailing-wire antenna

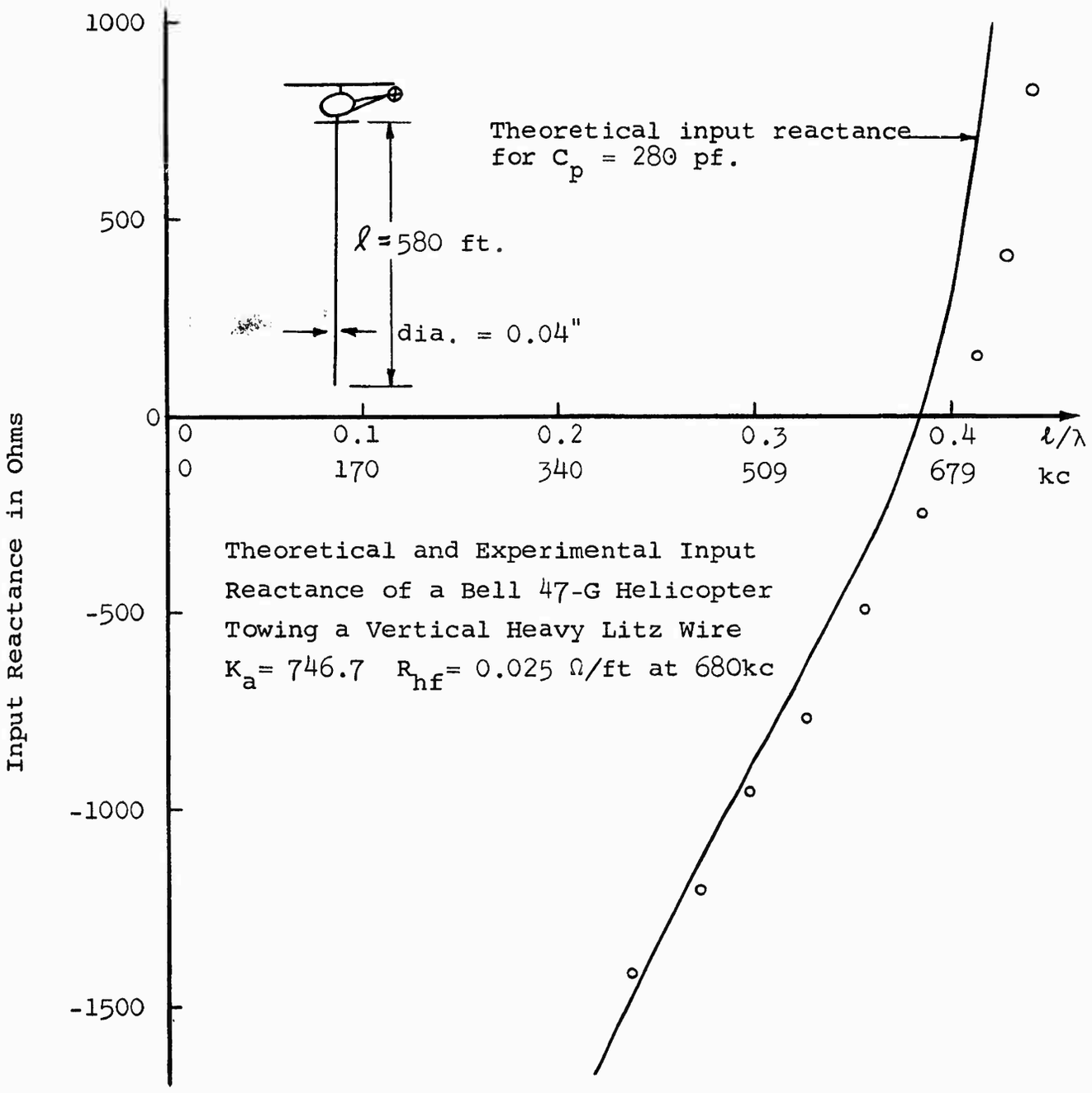

Figure 5. Theoretical and experimental input reactance of a 580-ft. trailing-wire antenna

Additional comparisons of theory and experiment are shown in Figures 6 through 9 for 1000-ft. lengths of solid phosphor-bronze and small litz wire, respectively. In each case the value of C_p is taken to be 280 pf. The general characteristics of these comparisons are similar to those of Figures 4 and 5; however, somewhat larger divergence can be seen between theoretical and experimental input impedance.

Although it is not likely that any practical VLF trailing-wire antenna will exceed $\lambda/2$ in length, it is worthwhile to consider the equivalent circuit and equation (10) for longer electrical lengths. Figures 10 and 11 show that the equivalent circuit and equation (10) are useful for electrical lengths at least up to $\ell/\lambda = 1$, especially for the prediction of input resistance.

Figures 12 and 13 show a comparison of theoretical and experimental input impedance for a moderately lossy carbon steel trailing-wire antenna. The measured resistance of this wire is 0.18 Ω/ft. at 400 kc. The effects of the ohmic losses predominantly alter the input resistance, but also lower the input reactance near half-wave antiresonance. Wire losses tend to raise the input resistance for low values of ℓ/λ, but they tend to lower it near antiresonance. Equation (10) predicts a zero value of input resistance for $\ell/\lambda = 0$, since the input impedance of a perfectly conducting wire must reduce to that of a pure capacitance at zero frequency. At zero frequency, the

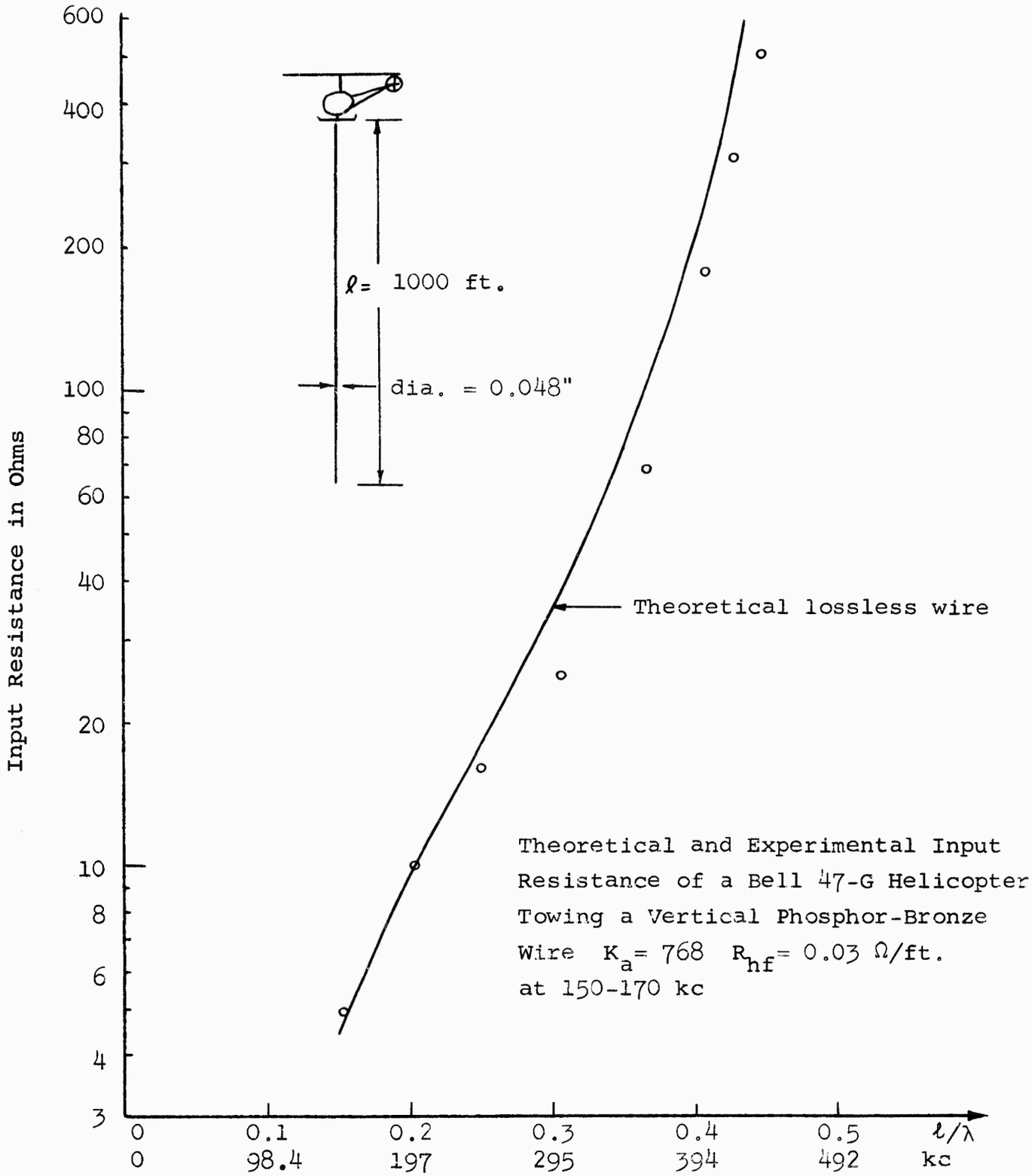

Figure 6. Theoretical and experimental input resistance of a 1000-ft. phosphor-bronze trailing-wire antenna

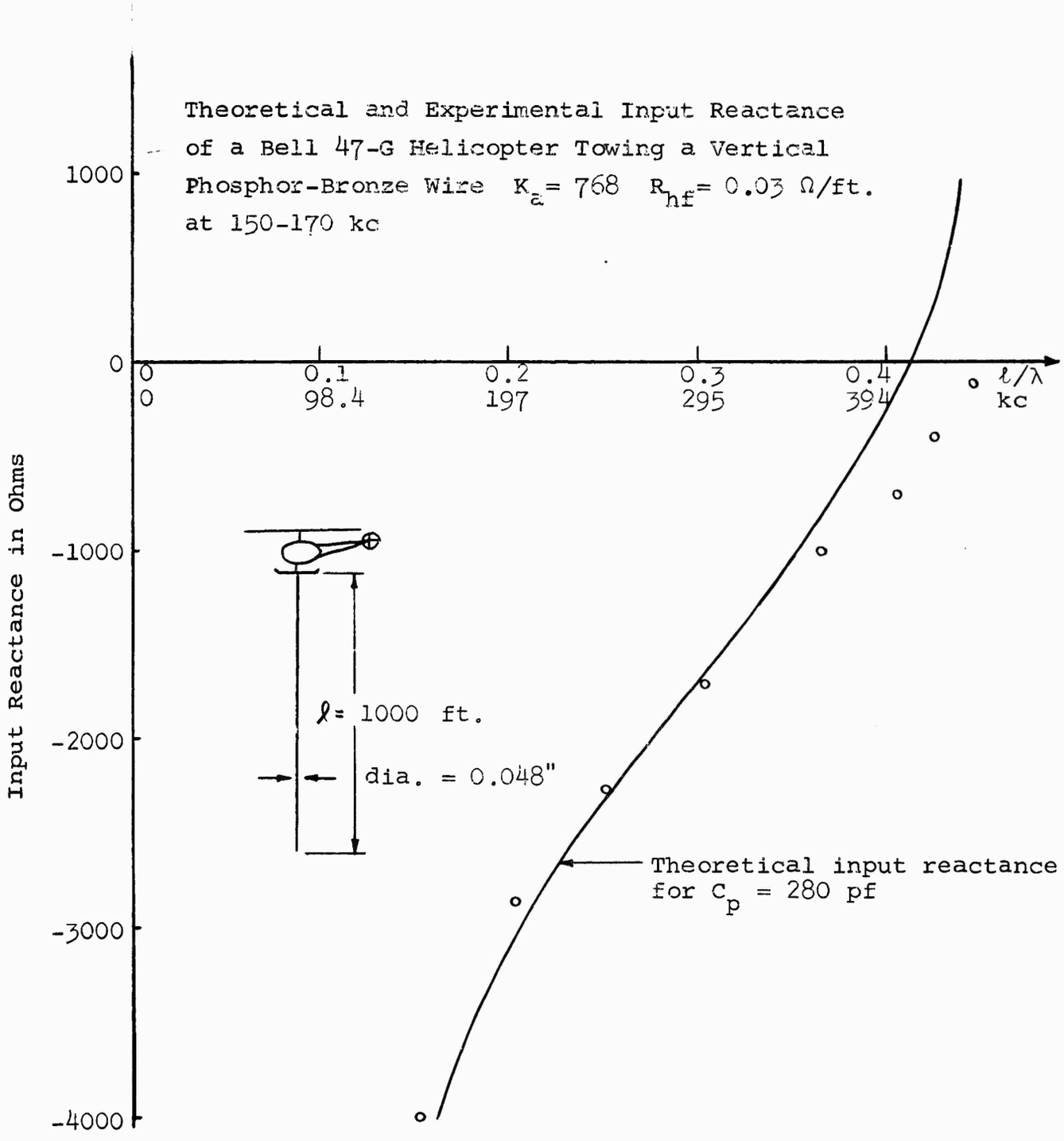

Figure 7. Theoretical and experimental input reactance of a 1000-ft. phosphor-bronze trailing-wire antenna

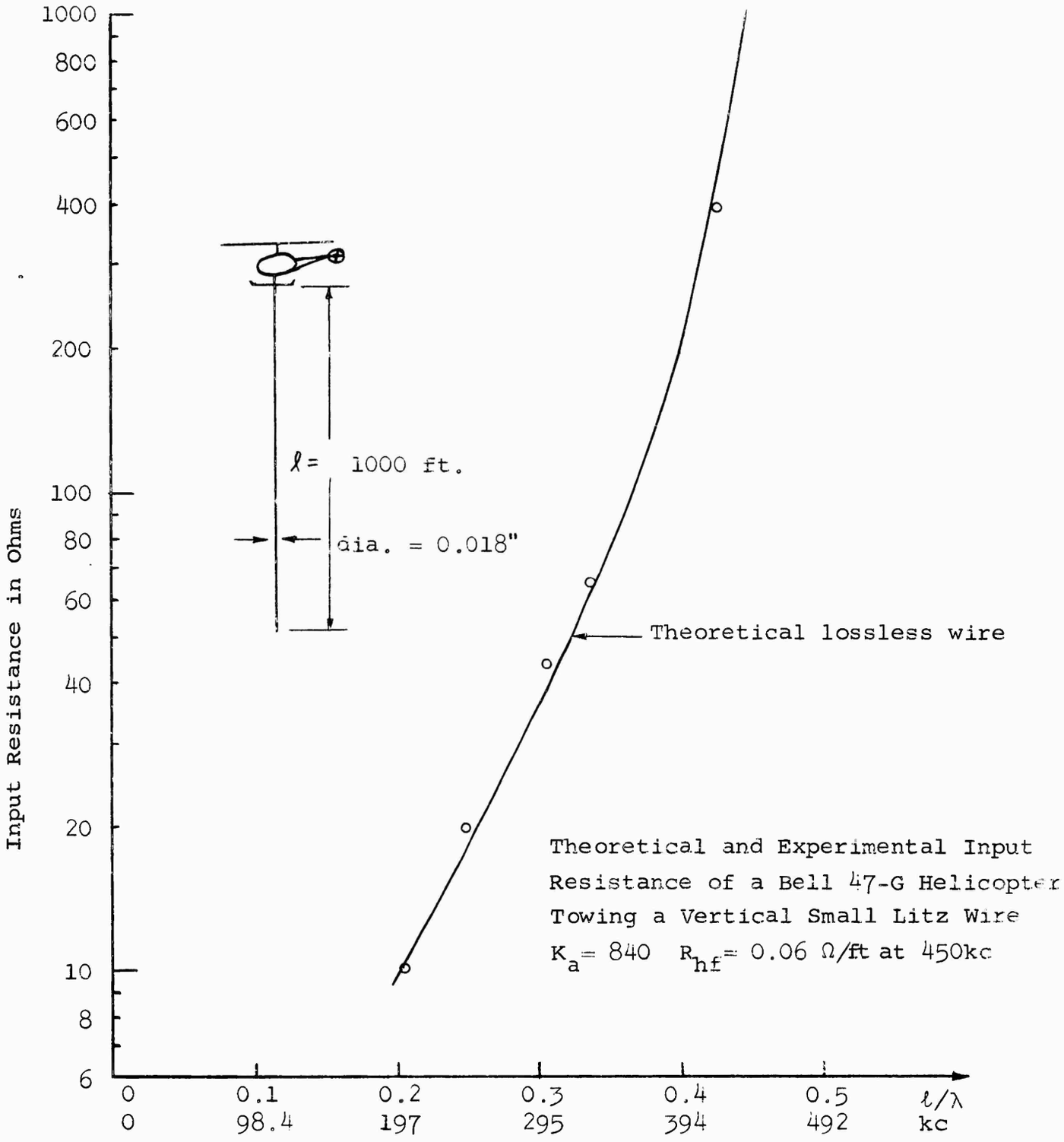

Figure 8. Theoretical and experimental input resistance of a 1000-ft. small litz wire trailing-wire antenna

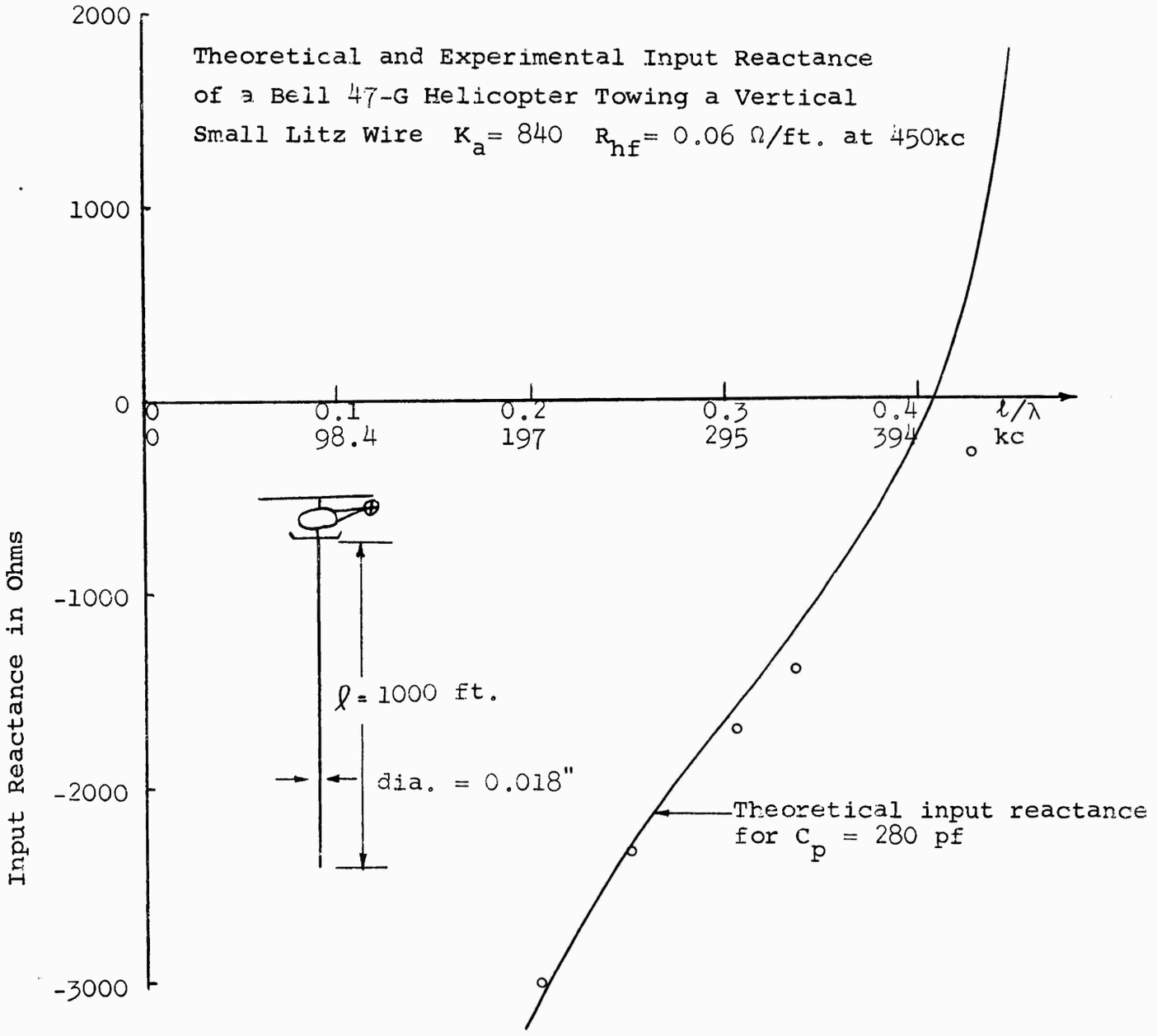

Figure 9. Theoretical and experimental input reactance of a 1000-ft. small litz wire trailing-wire antenna

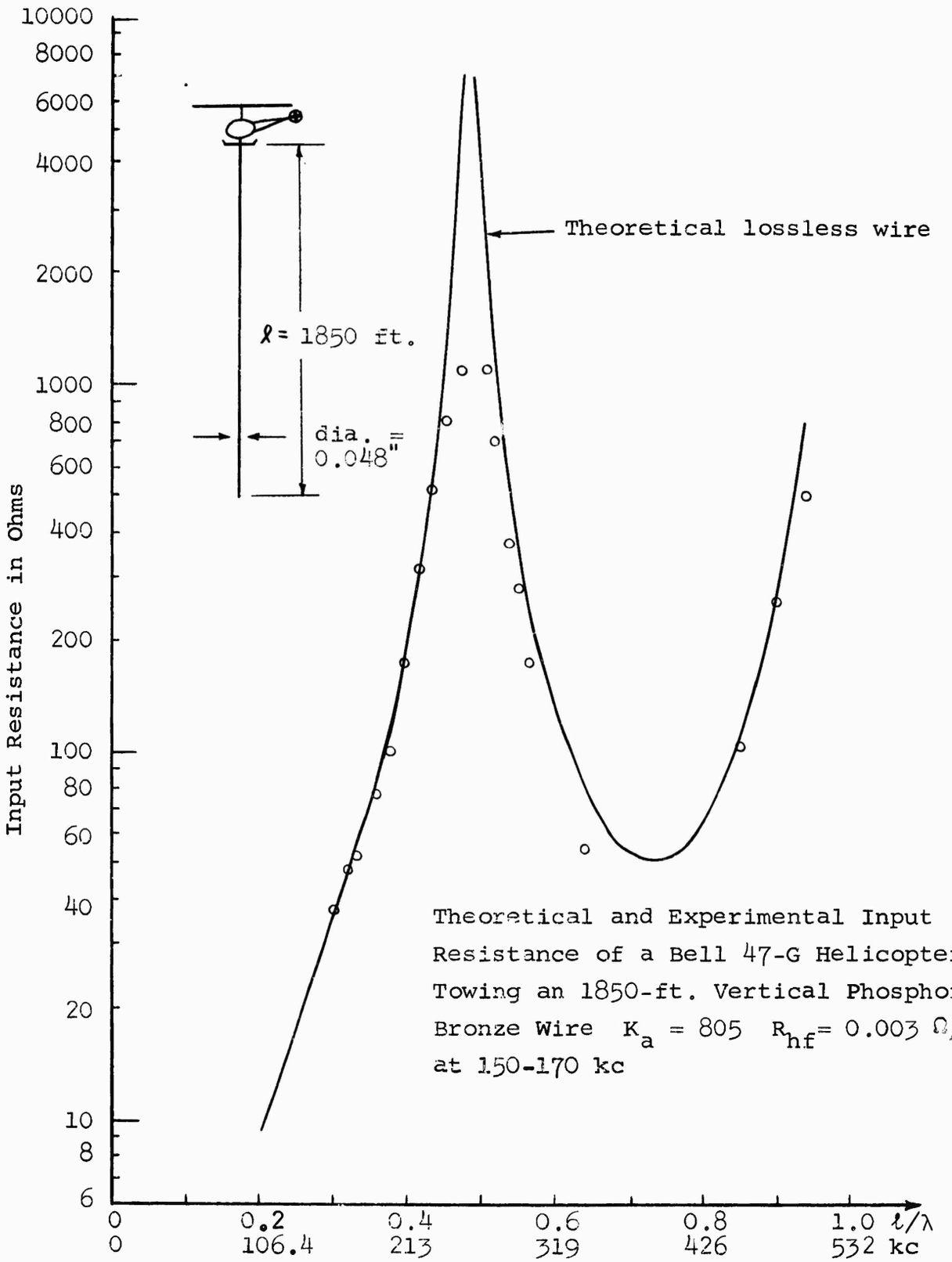

Theoretical and Experimental Input Resistance of a Bell 47-G Helicopter Towing an 1850-ft. Vertical Phosphor-Bronze Wire $K_a = 805$ $R_{hf} = 0.003$ Ω/ft. at 150-170 kc

Figure 10. Theoretical and experimental input resistance of an 1850-ft. phosphor-bronze trailing-wire antenna

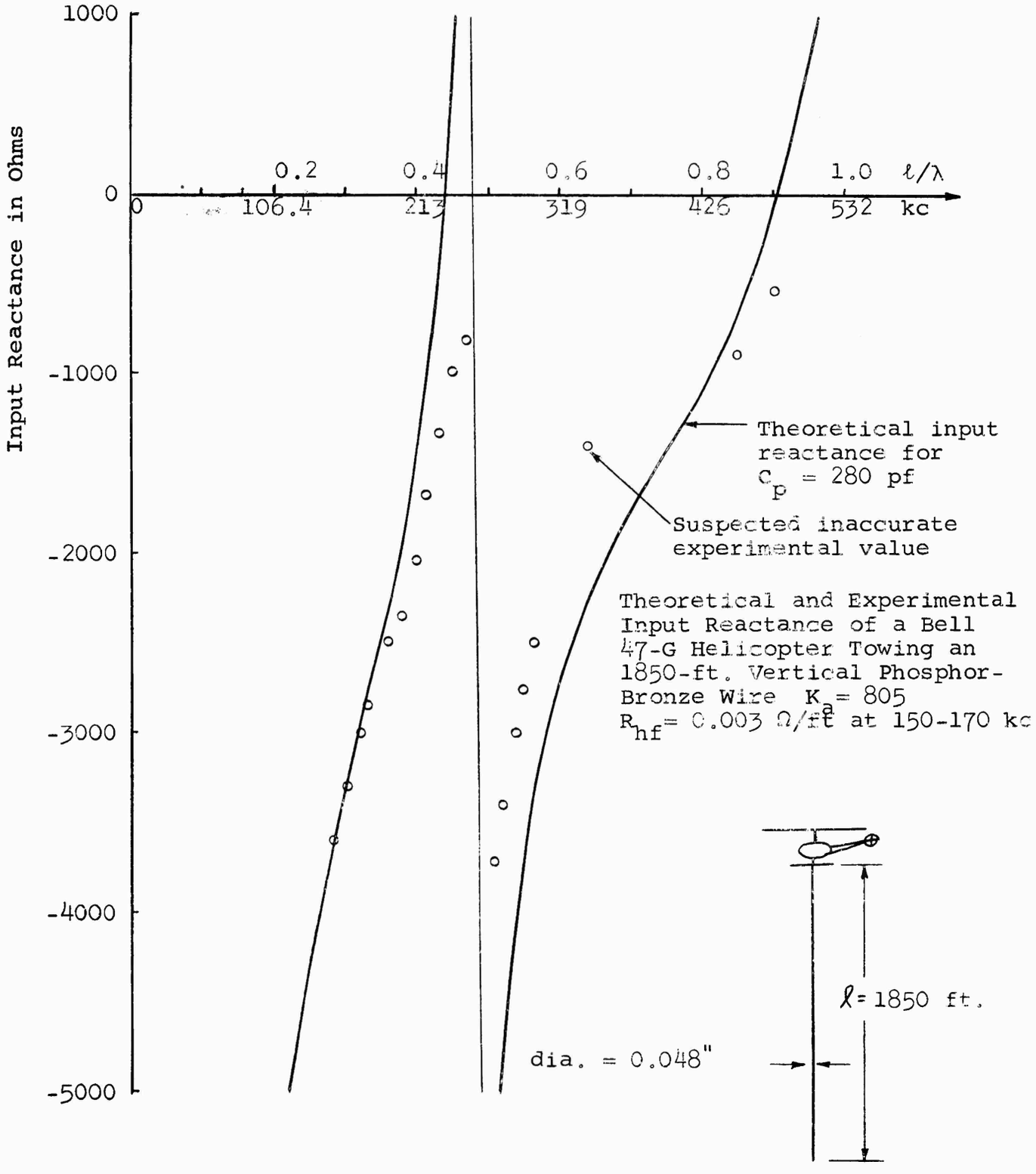

Figure 11. Theoretical experimental input reactance of an 1850-ft. phosphor-bronze trailing-wire antenna

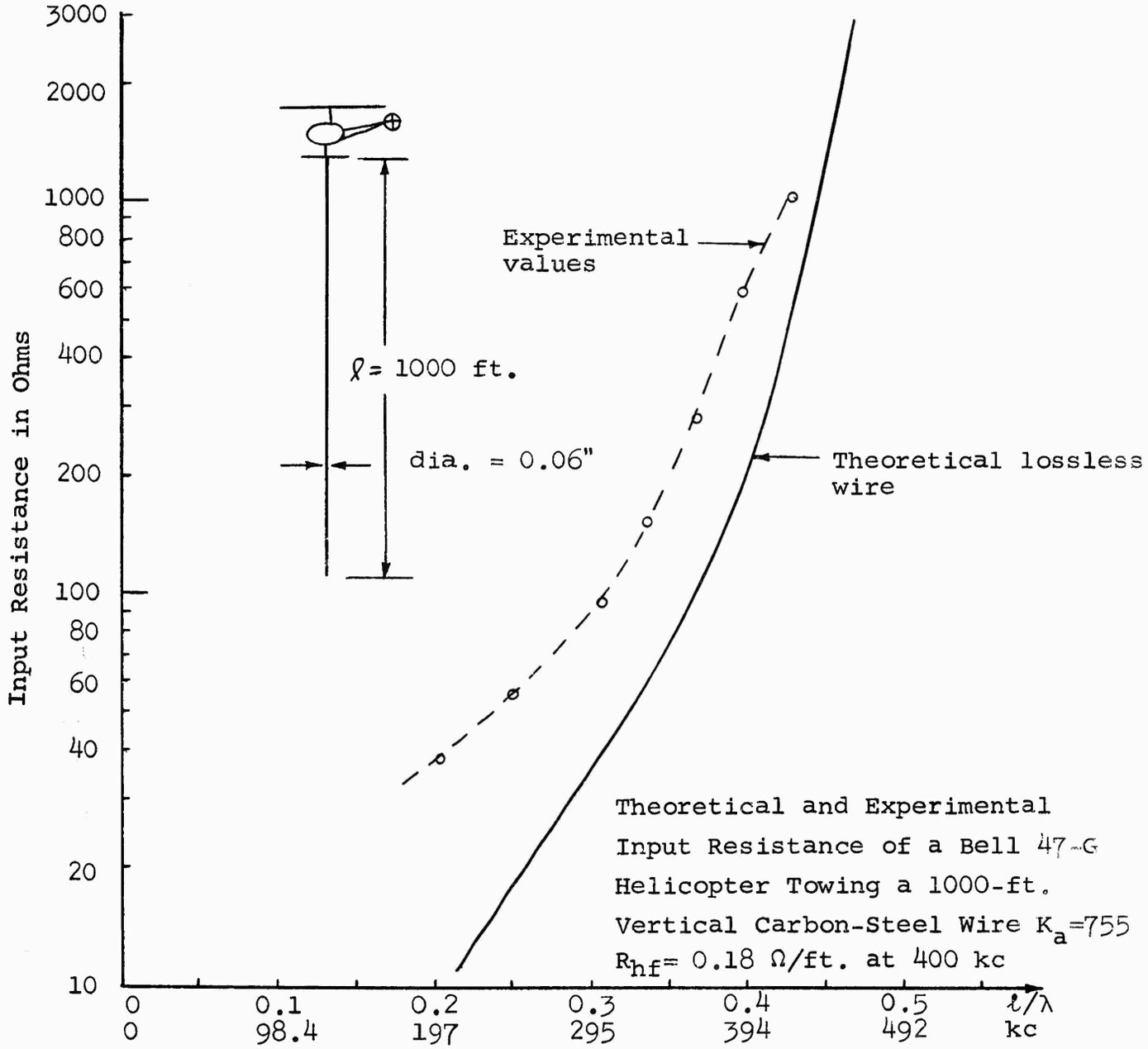

Figure 12. Theoretical and experimental input resistance of a lossy carbon-steel trailing-wire antenna

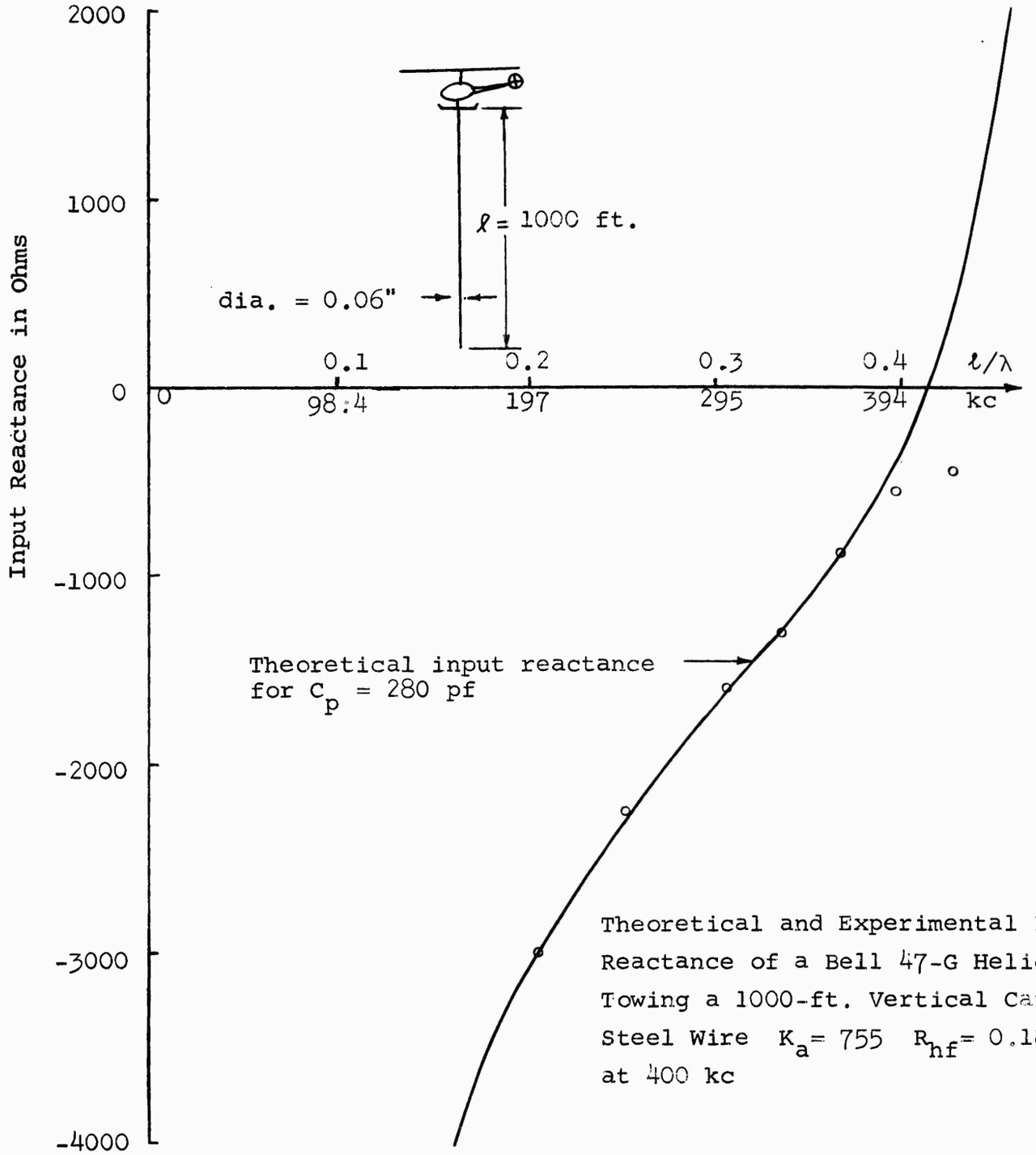

Figure 13. Theoretical and experimental input reactance of a lossy carbon-steel trailing-wire antenna

measured value of input resistance is zero also, since no charges are in motion. However, at some very low frequency the lossy antenna would have an appreciable resistance due to ohmic losses alone. The manner in which the input resistance of a lossy trailing-wire antenna approaches zero as $\ell/\lambda \to 0$ is not that expressed by (10); however the actual behavior near $\ell/\lambda = 0$ is not known.

The previous comparisons of theory and experiment are for antennas which are too short to be practical for use in the VLF spectrum. Their primary purpose in this report is to instill confidence in the theoretical model. We now use (10) to compute input impedance characteristics of VLF trailing-wire antennas. Only the impedance of the wires is computed, since the value of C_p will vary with the type of aircraft. Figures 14 and 15 show theoretical input impedance characteristics for three 0.1-inch diameter wires of length 10,000, 15,000 and 25,000 feet, respectively. The impedance characteristics are shown only over a range $0 \leq \ell/\lambda \leq 0.45$ for each wire since this is the most likely range of electrical lengths for practical VLF antennas. The wire material is 30%-conductivity solid copperweld with a dc-resistance of 0.00349 Ω/ft. A commercially available wire which should be usable to obtain these characteristics is AWG B$\acute{\text{e}}$S No. 10 30%-conductivity solid copperweld. Specifications for this wire are: diameter = 0.1019 in., weight = 28.81 lbs/1000 ft, resistance = 0.003396 Ω/ft, and breaking load = 1231 lbs [7].

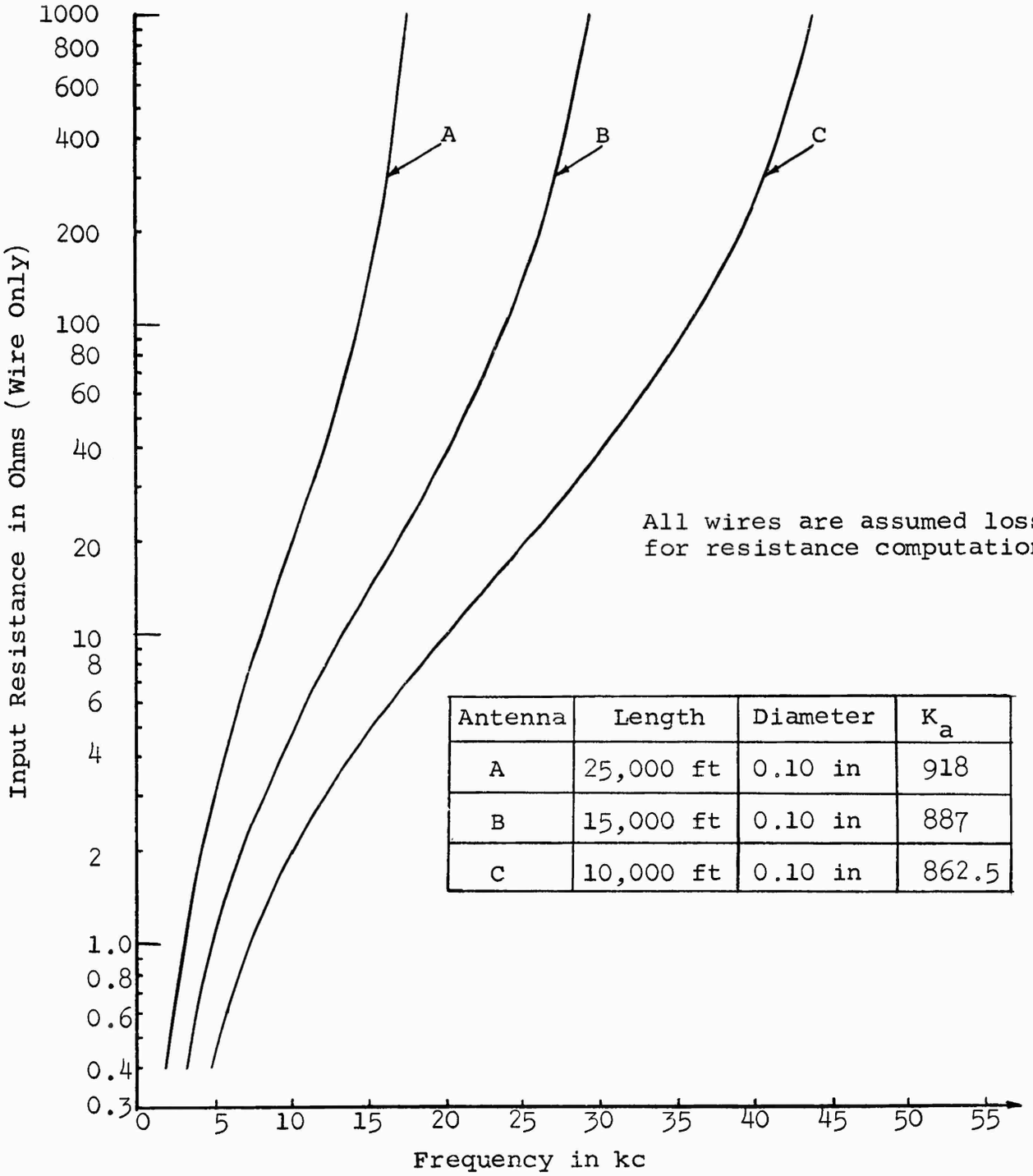

Antenna	Length	Diameter	K_a
A	25,000 ft	0.10 in	918
B	15,000 ft	0.10 in	887
C	10,000 ft	0.10 in	862.5

Figure 14. Theoretical input resistance of selected VLF trailing-wire antennas

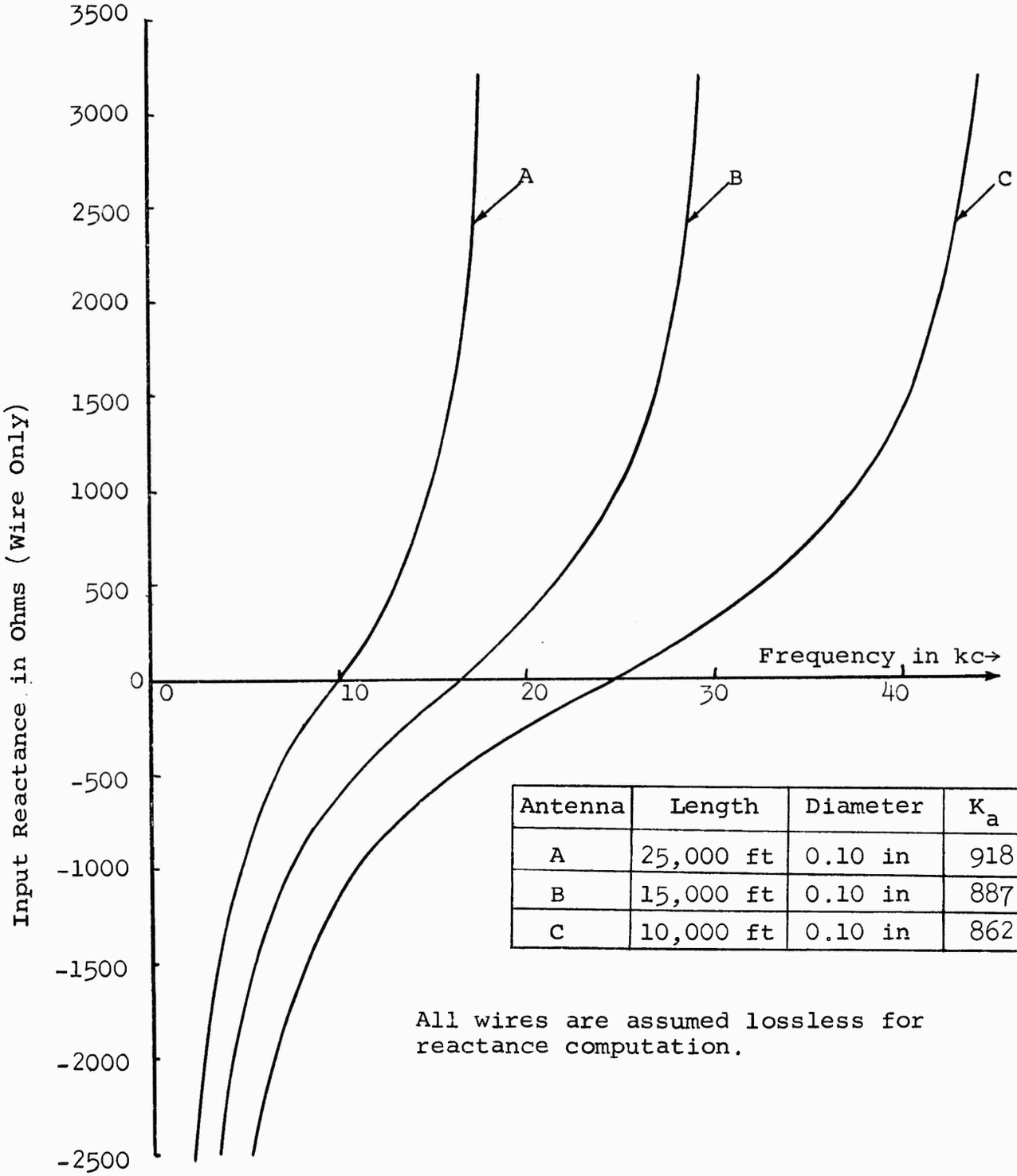

Antenna	Length	Diameter	K_a
A	25,000 ft	0.10 in	918
B	15,000 ft	0.10 in	887
C	10,000 ft	0.10 in	862.5

All wires are assumed lossless for reactance computation.

Figure 15. Theoretical input reactance of selected VLF trailing-wire antennas

3.0 RADIATION EFFICIENCY OF VLF TRAILING-WIRE ANTENNAS

3.1 A Method for the Calculation of Radiation Efficiency

It is well known that electrically short antennas are generally not as efficient radiators as longer ones because of their smaller dipole moment, resulting in a larger proportion of input power being dissipated in heating up the antenna conductors (ohmic losses). Airborne VLF antennas are likely to be electrically short, and if they are to radiate large amounts of power, radiation efficiency is of prime importance.

If one could determine the true current distribution on a trailing-wire antenna, one could then determine the far-zone fields and find the radiated power by integrating the Poynting vector over an infinite sphere enclosing the antenna. The ohmic power losses could be determined by integrating $I^2(x)R$ (where R = ohmic resistance per unit length) over the length of the wire. To the author's knowledge, the true current distribution on a trailing-wire antenna is not known; hence one must resort to approximations. The approximate method to be used here is as follows: As shown by Figures 4, 6, 8, and 10, the input resistance of a low-loss trailing-wire antenna of length $\ell \leq \lambda/2$ differs appreciably from that of a perfectly conducting antenna only near $\ell/\lambda = 0$ and $\ell/\lambda = 0.5$. Consequently, it can be assumed that R_r, the radiation resistance due to radiated power, is relatively unaffected by small ohmic losses [8]. Since the antenna is very long and thin, it is reasonable

to assume that a sinusoidal current distribution exists on the antenna [9]. The radiated power is then given by $P_r = I_{in}^2 R_r$, where P_r = radiated power in watts, I_{in} = rms input current in amperes, and R_r is the radiation resistance in ohms, given to a good approximation by the real part of (10). The ohmic power losses are calculated by integrating $I^2(x)R$ over the length of the wire, using the assumed sinusoidal current distribution. The radiation efficiency is then given by

$$\text{Eff in } \% = \frac{P_r}{P_r + P_L} \times 100 \ , \qquad (13)$$

where P_L is the total average ohmic power loss in watts. This method is somewhat analogous to that used in computing the losses in the walls of copper-plated waveguides [10]; wherein the enclosed fields are found by assuming perfectly conducting walls, and the losses are then found by integrating the I^2R losses over the walls. The distribution of current in the walls is taken to be that which would exist if the walls were perfectly conducting.

Let us consider a wire with an assumed current distribution as shown in Figure 16:

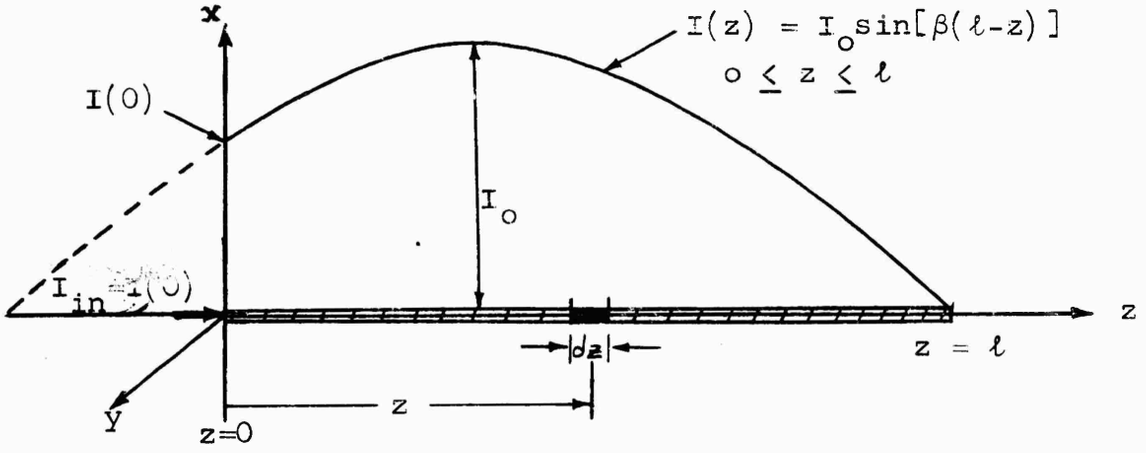

Figure 16. Approximate current distribution on a trailing-wire antenna.

We assume that a monochromatic source of angular frequency ω radians/sec supplies current to the antenna. Then

$$i(z,t) = I_o \sin[\beta(\ell - z)] \sin \omega t \qquad 0 \leq z \leq \ell. \quad (14)$$

The system is assumed to be in steady-state operation. The instantaneous power lost in heat in any segment of wire of length dz is $dp_L(t,z) = i^2(z,t)Rdz$, where R is the ac ohmic resistance per unit length of the wire. The total instantaneous ohmic power loss is given by

$$p_L(t) = \int_0^{\ell} i^2(z,t)Rdz = I_o^2 R \sin^2(\omega t) \int_0^{\ell} \sin^2[\beta(\ell - z)]dz. \quad (15)$$

Integration of (15) gives

$$p_L(t) = I_o^2 R \sin^2(\omega t)\left[\frac{\ell}{2} - \frac{\lambda}{8\pi} \sin(4\pi\ell/\lambda)\right]. \quad (16)$$

The average ohmic power loss is then

$$P_L = \frac{1}{2T} \int_{-T}^{+T} p_L(t)dt = \frac{I_o^2 R}{2T}\left[\frac{\ell}{2} - \frac{\lambda}{8\pi} \sin(4\pi\ell/\lambda)\right] \int_{-T}^{+T} \sin^2(\omega t)dt, \quad (17)$$

where $T = \frac{2\pi}{\omega}$.

Integration of (17) gives

$$P_L = \frac{I_o^2 R}{2}\left[\frac{\ell}{2} - \frac{\lambda}{8\pi} \sin(4\pi\ell/\lambda)\right] \text{ watts}. \quad (18)$$

The instantaneous radiated power is given by

$$p_r(t) = i^2(t,0)R_r = R_r I_o^2 \sin^2(\beta\ell)\sin^2(\omega t). \quad (19)$$

The average radiated power is given by

$$P_r = \frac{1}{2T}\int_{-T}^{+T} p_r(t)\,dt = \frac{R_r I_o^2}{2T}\sin^2(\beta\ell)\int_{-T}^{+T}\sin^2(\omega t)\,dt. \quad (20)$$

Integration of (20) gives

$$P_r = \frac{I_o^2 R_r}{2}\sin^2(2\pi\ell/\lambda) \text{ watts}. \quad (21)$$

Substitution of (18) and (21) into (13) gives

$$\text{Eff in } \% = \frac{R_r \sin^2(2\pi\ell/\lambda)}{R_r\sin^2(2\pi\ell/\lambda) + R\left[\frac{\ell}{2} - \frac{\lambda}{8\pi}\sin(4\pi\ell/\lambda)\right]} \times 100, \quad (22)$$

where R_r is the real part of (10). The quantity R is a function of λ and can be determined from the conventional skin effect equations [10, p. 247]:

$$R = \frac{R_s}{\sqrt{2}\,\pi a}\left\{\frac{\text{Berq Bei'q - Beiq Ber'q}}{(\text{Ber'q})^2 + (\text{Bei'q})^2}\right\} \frac{\text{ohms}}{\text{unit length}} \quad (23)$$

where

$$R_s = \frac{1}{\sigma\delta} = \sqrt{\frac{\pi f\mu}{\sigma}}\,, \quad q = \frac{\sqrt{2}\,a}{\delta} \text{ and } \delta = \frac{1}{\sqrt{\pi f\mu\sigma}}\,. \quad (24)$$

In (23)

$$\text{Berq} + j\text{Beiq} = J_o(j^{-\frac{1}{2}}q), \quad (25a)$$

and

$$\text{Ber'q} + j\text{Bei'q} = \frac{d}{dq}[\text{Berq} + j\text{Beiq}] = j^{-\frac{1}{2}}J_o'(j^{-\frac{1}{2}}q). \quad (25b)$$

In equations (23) through (25b)

R_s = surface resistivity in ohms per square

a = wire radius in meters

σ = wire conductivity in mhos/meter

δ = skin depth in meters

f = frequency in cycles per second

μ = permeability in henrys/meter

and

$J_o(v)$ = Bessel function of first kind, zero order, and of argument v.

The quantity R may also be calculated by means of

$$R = \frac{R_s}{\sqrt{2}\ \pi a} \frac{M_o(q)}{M_1(q)} \sin\left\{\theta_1(q) - \theta_o(q) - \frac{\pi}{4}\right\} \qquad (26)$$

where

$$M_o(q)e^{j\theta_o(q)} = J_o(qj^{3/2}) = \text{berq} + \text{jbeiq} \qquad (27a)$$

and

$$M_1(q)e^{j\theta_1(q)} = J_1(qj^{3/2}) = \text{ber}_1 q + \text{jbei}_1 q. \qquad (27b)$$

Equation (23) is useful when tables of the Berq, Beiq, Ber'q and Bei'q functions are available [11]. Equation (26) is more convenient for computation when tables of $M_o(q)$, $M_1(q)$, $\theta_o(q)$, and $\theta_1(q)$ are available [12].

Equation (22) should give reasonably accurate values of radiation efficiency except near $\ell/\lambda = 0$ and $\ell/\lambda = 0.5$. Near $\ell/\lambda = 0$ the effective ohmic resistance becomes much larger than the radiation resistance as given by (10); consequently the losses are no longer a small perturbation in the system. The division of input power between ohmic power losses and

radiated power becomes a complicated relation involving not only the principal wave (quasi - TEM mode) but also higher order modes not accounted for by (10). Fortunately, antennas operated near $\ell/\lambda = 0$ are of little practical interest. For $\ell/\lambda = 0.5$ equation (14) gives a zero value for the input current. For a finite source voltage, this would imply that the input resistance of a thin end-fed half-wave antenna with a sinusoidal current distribution is infinite and that no power can be transferred into it. It is known that the input resistance of a thin full-wave dipole antenna can be large (~ 10,000 ohms), but that infinite input resistance can occur only if the antenna is infinitesimally thin, i. e., $\ell/a = \infty$ and hence $K_a = \infty$. Figure 17 illustrates the actual behavior of the current distribution on a thin full-wave cylindrical antenna [9, p. 240].

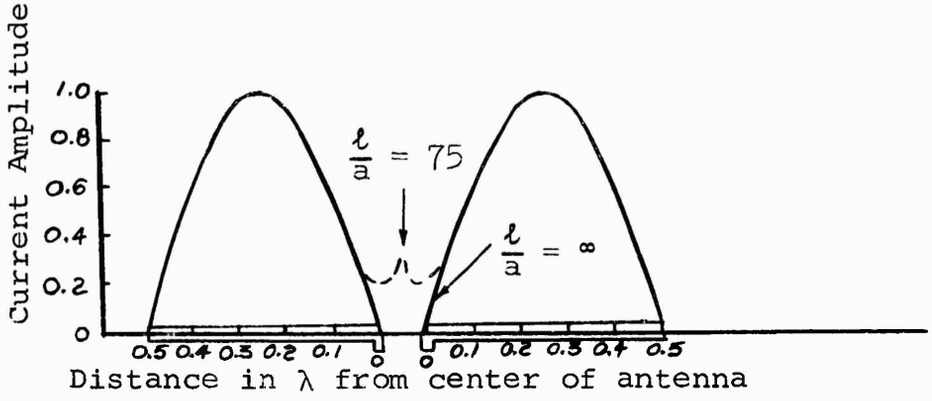

Figure 17. Current distribution on a thin full-wave cylindrical antenna.

For the case of a trailing-wire antenna operating near $\ell/\lambda = 0.5$, the input current will have some small, non-zero value, since no actual wire is infinitesimally thin. The use of (14) in the calculation of ohmic power losses near $\ell/\lambda = 0.5$ will give somewhat lower losses than actually exist; however it is not practical to estimate the magnitude of the error as it will vary with each antenna. This error may be insignificant in any case since (10) does not accurately give the value of R_r near $\ell/\lambda = 0.5$, even for a low-loss trailing-wire antenna.

3.2 Numerical Calculations for Selected VLF Trailing-Wire Antennas

Keeping the above restrictions in mind, we proceed now to calculate the radiation efficiency of the antennas for which theoretical impedance characteristics are given in Figures 14 and 15. Let us divide (26) by R_o, the dc ohmic resistance per unit length, where

$$R_o = \frac{1}{\pi a^2 \sigma} . \tag{28}$$

Substitution of (24) into the result gives

$$\frac{R}{R_o} = \frac{q}{2} \frac{M_o(q)}{M_1(q)} \sin \left[\theta_1(q) - \theta_o(q) - \frac{\pi}{4}\right] . \tag{29}$$

The conductivity of 30%-conductivity copperweld is $\sigma = 1.725 \times 10^7$ mhos/meter. Then for a 0.1-inch diameter wire,

$$R_o = \frac{1}{\pi a^2 \sigma} = \frac{1}{(3.142)(1.27\times10^{-3})^2(1.725\times10^7)}$$

$$= 0.01145 \frac{\text{ohms}}{\text{meter}} = 0.00349 \frac{\text{ohms}}{\text{ft.}} .$$

Values of R_r taken from Figure 14 and values of R computed from (29) are substituted into (22) to give the radiation efficiency curves shown in Figure 18. The curves of Figure 18 are drawn for $0 \leq \ell/\lambda \leq 0.48$ for each wire. Although it is not shown in Figure 18, the radiation efficiency will have a maximum somewhere near $\ell/\lambda = 0.5$. Unfortunately, in this region of ℓ/λ the approximate expression (22) becomes inaccurate. Near $\ell/\lambda = 0.5$ the theoretical values given by (22) will be too high because the actual antenna resistances will be less than the values of R_r given by the real part of (10).

From (22) and Figure 18 it can be seen that for a given wire diameter and the same electrical length, the longer wires are less efficient than the shorter wires. The reason for this is that ohmic losses are directly proportional to physical length, while the radiation resistance given by (10) is relatively insensitive to length (since $K_a = 60[\ln(\frac{2\ell}{a}) - 1]$), except near $\ell/\lambda = 0.5$. It is obvious that higher efficiencies are obtained when R_r is large and R is small. These two conditions imply that the most efficient trailing-wire antenna for a given frequency is a wire of very good conductivity operated near $\ell/\lambda = 0.5$; however physical length constraints and input reactance requirements may dictate other operating points.

Antenna	Length	Diameter	K_a
A	25,000 ft	0.10 in	918
B	15,000 ft	0.10 in	887
C	10,000 ft	0.10 in	862.5

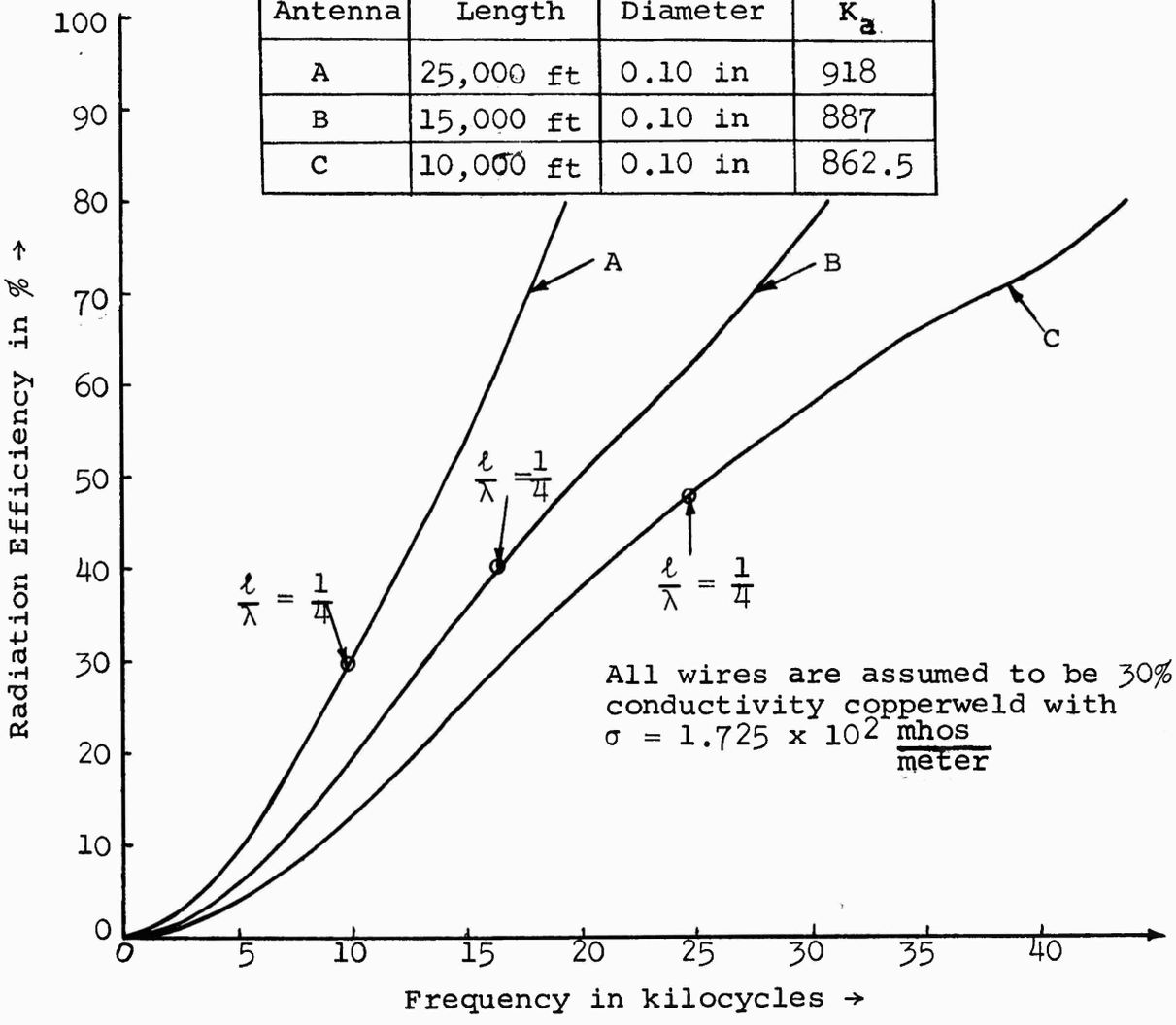

Figure 18. Theoretical radiation efficiency of selected VLF trailing-wire antennas

4.0 COMPARISON OF IMPEDANCE AND RADIATION EFFICIENCY OF VLF TRAILING-WIRE AND TRANSMISSION-LINE ANTENNAS

It has been shown by R. W. Kulterman [2] that the side-loaded transmission line shown in Figure 19 can operate in an antenna mode and that it is equivalent to a multiply-fed cylindrical antenna as far as its radiating properties are concerned.

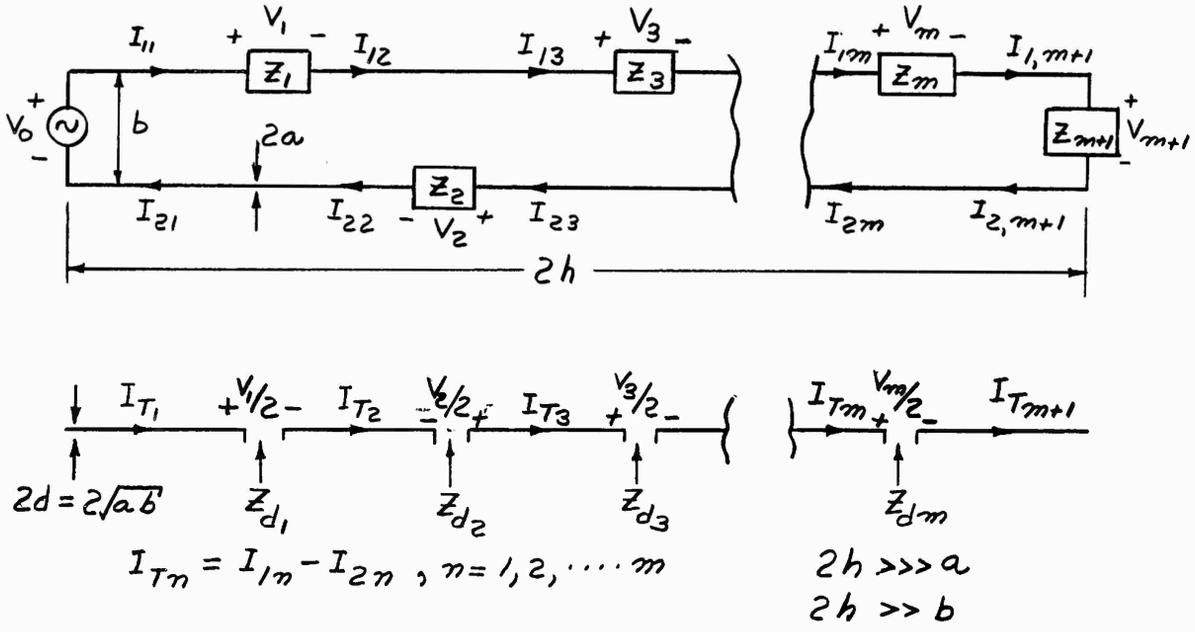

Figure 19. General side-loaded transmission-line antenna and equivalent cylindrical antenna.

For the VLF airborne antenna application, only the types shown in Figure 20 will be considered. Investigation has shown that these three types possess most of the desirable features of the general case (at least for electrically-short antennas), and that there is little to be gained practically by the use of more than two lumped impedances.

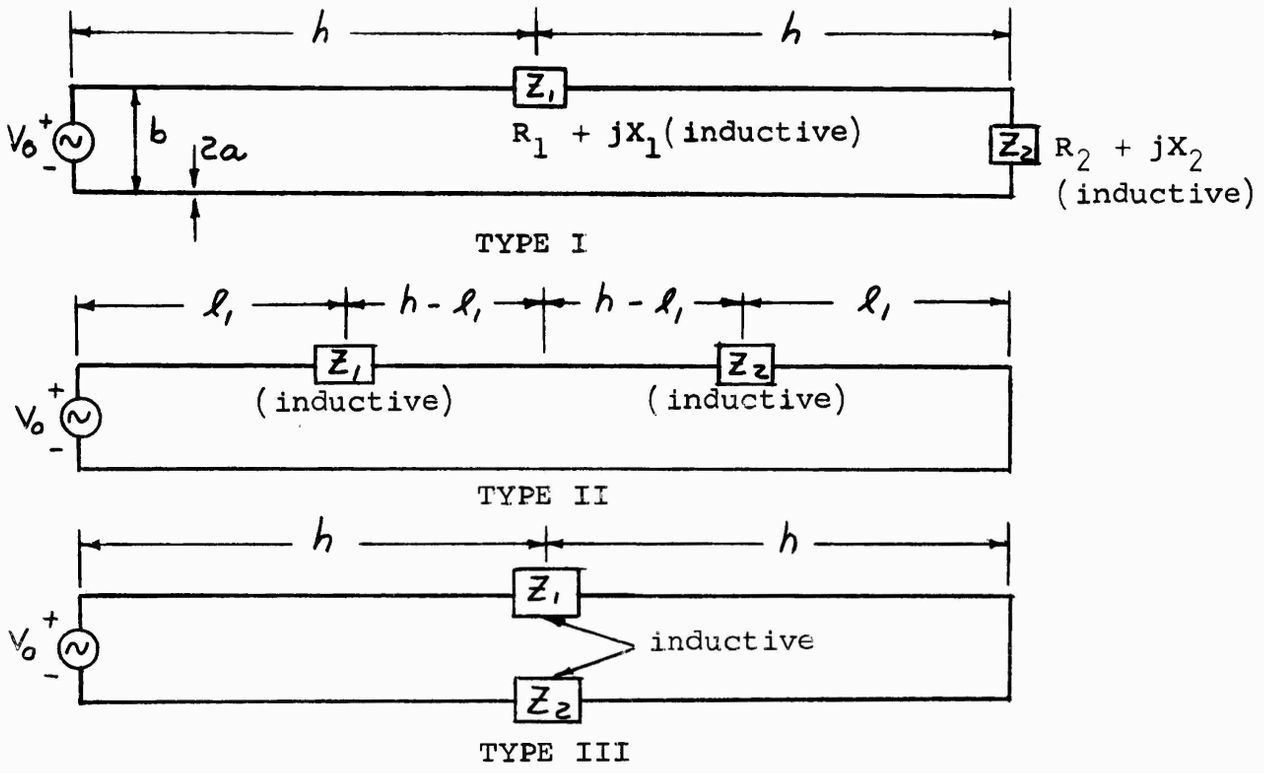

Figure 20. Three types of side-loaded transmission-line antennas.

Kulterman has also shown that, assuming lossless wires, the input impedance and radiation efficiency characteristics of a side-loaded transmission-line antenna can be computed from the general equivalent circuit of Figure 21. If one considers

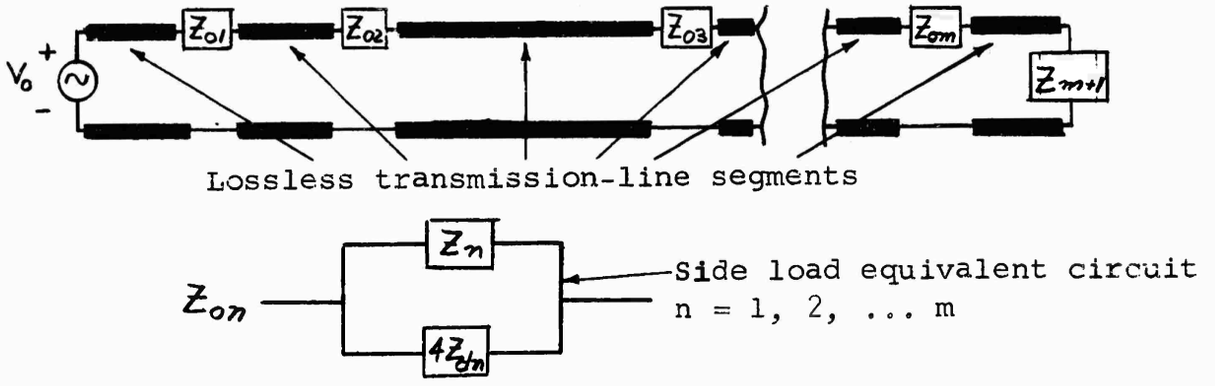

Figure 21. Equivalent circuits of general side-loaded transmission-line antenna and side-loads.

transmission lines with low ohmic losses, the form of the equivalent circuit and the equations for input impedance remain the same, except that the characteristic impedance of line becomes that of a lossy line. The quantities Z_{dn} are the input impedances of the multiply-fed cylindrical antenna. The method for the computation of Z_{dn} for the general case is complex, and will not be given here. The method is given in detail in Appendices A and B of [2, pp. 165-170]. Fortunately, for the electrically short antennas of Figure 20, the computation of Z_{dn} is relatively easy.

We now proceed to calculate the input impedance and radiation efficiency characteristics for representative examples of a Type I transmission-line antenna. For the transmission-line antennas it is assumed that the wires are perfectly conducting and that the only ohmic losses in the antenna are due to the finite Q of the lumped impedances. This assumption is questionable for physically long antennas; however it simplifies the computations enormously, and at least gives us an upper bound on the radiation efficiency. Kulterman has derived expressions for the input impedance and radiation efficiency of a Type I antenna. The equations are complex and the reader is referred to [2, p. 69-70] for the equations and the design procedure. The first example of a Type I antenna is shown schematically in Figure 22.

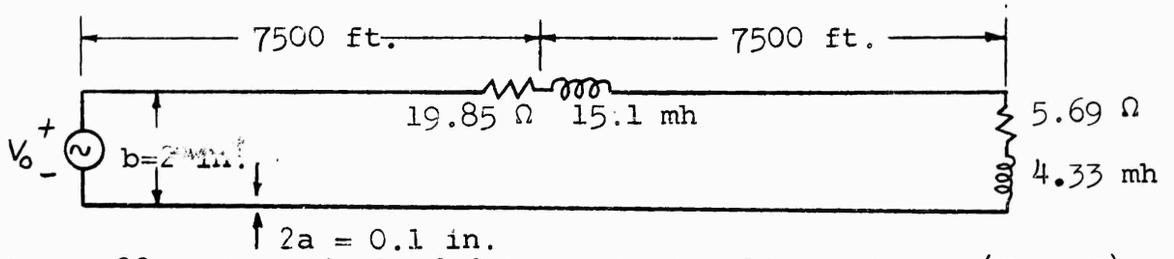

Figure 22. VLF side-loaded transmission-line antenna (Type I).

The resistances in the lumped impedances represent the resistance due to the finite Q of the inductors. In this example, both inductors were arbitrarily assumed to have Q = 100 at 21 kc, and the resistance is assumed to remain constant over the frequency range of interest. Input impedance and radiation efficiency characteristics for this antenna are shown in Figures 23 and 24. If zero input reactance is an important requirement, it can be seen that a desirable operating point for this antenna is at 18.2 kc, where $R_{in} = 35\Omega$, $X_{in} \approx 0$ and efficiency = 3%. It should be remembered at this point that this efficiency is only an upper bound on the efficiency, since ohmic losses in the wires have been neglected. The true radiation efficiency is less than 3% at 18.2 kc.

In an effort to obtain a higher efficiency near 18 kc, the transmission-line antenna of Figure 25 was designed.

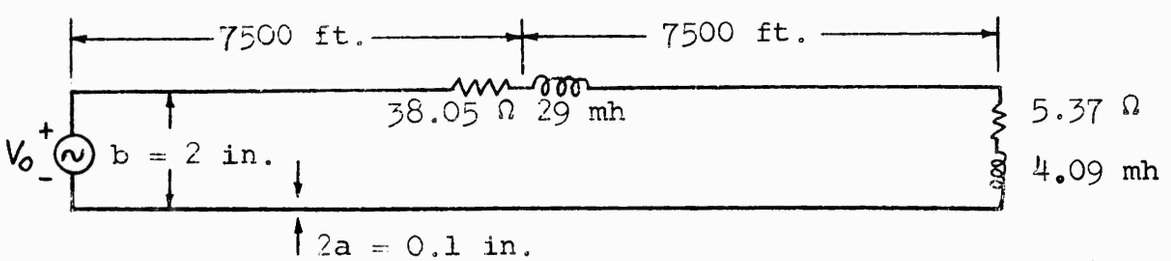

Figure 25. VLF side-loaded transmission-line antenna (Type I)

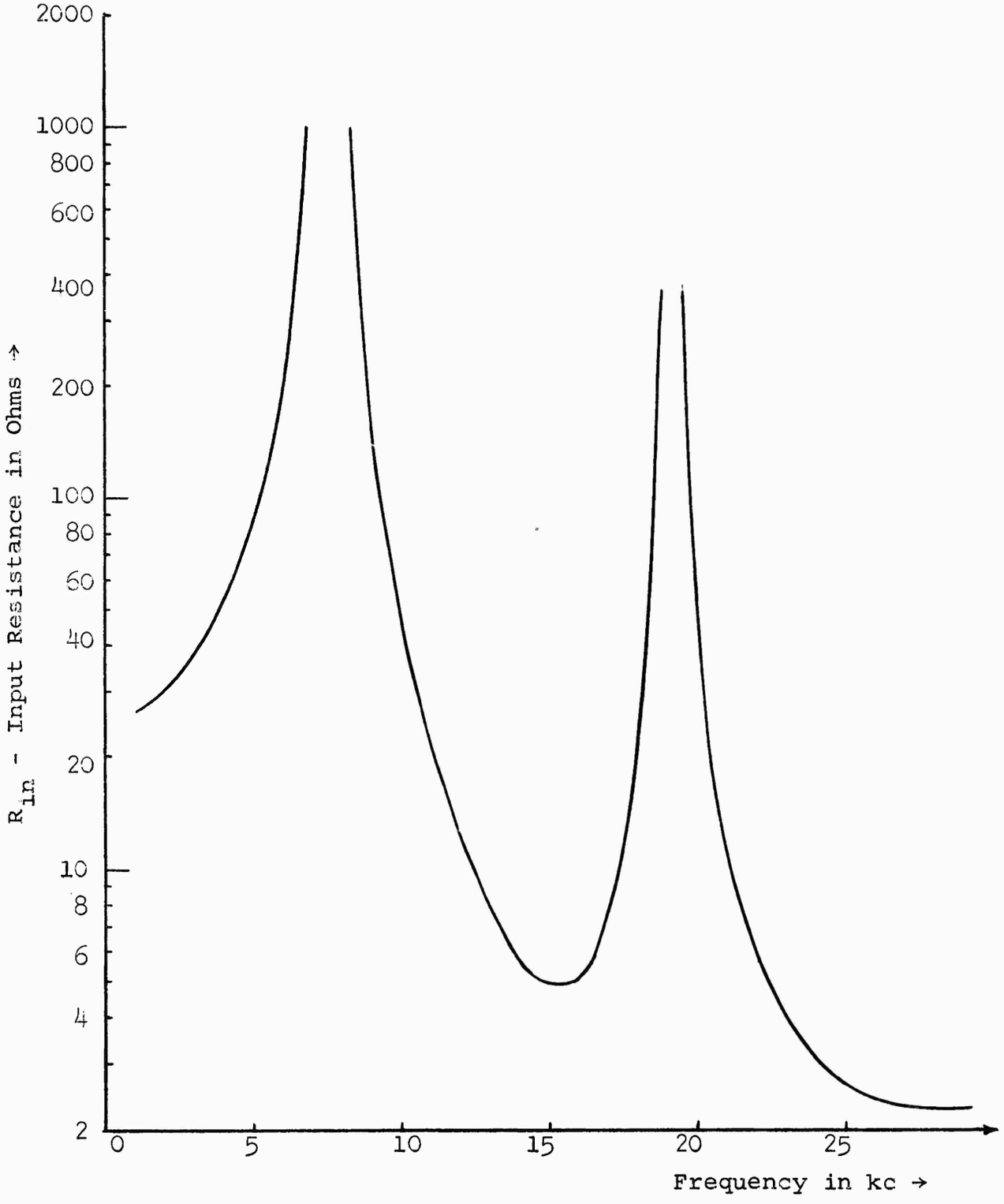

Figure 23. Theoretical input resistance of the Type I transmission-line antenna of Figure 22

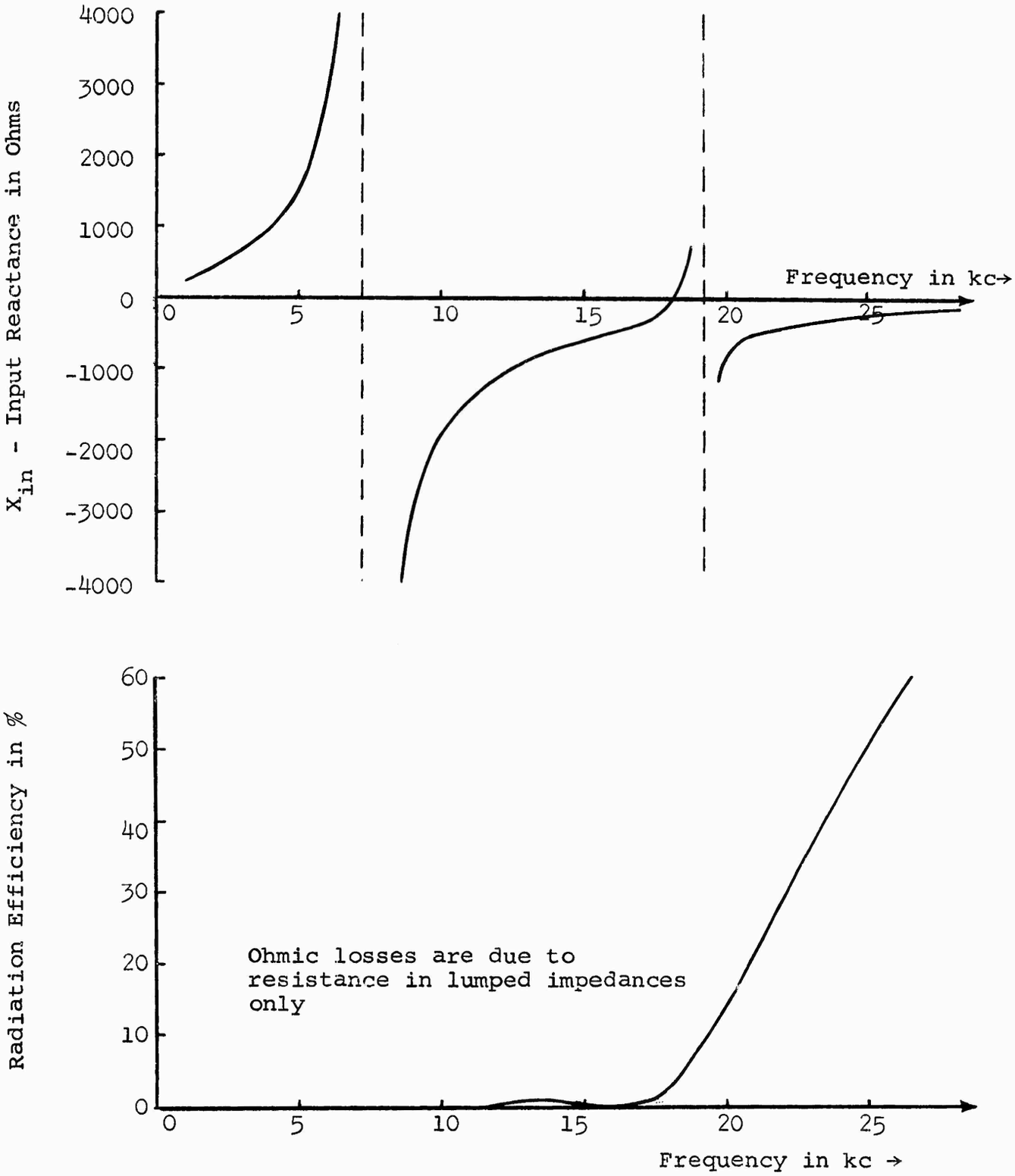

Figure 24. Theoretical input reactance and radiation efficiency of the Type I transmission-line antenna of Figure 22

Input impedance and radiation efficiency characteristics for this antenna are shown in Figures 26 and 27. At the same operating frequency (18.2 kc) we have $R_{in} \approx 250\Omega$, $X_{in} = 0$ and efficiency = 11%. The efficiency at the zero reactance point has been increased; however, the operating point is now in a region with a high rate of change of input resistance with respect to frequency.

An antenna of Type II is shown schematically in Figure 28. Theoretical equations for impedance and efficiency are given in [2, p. 90-92]. In this example the resistances were determined

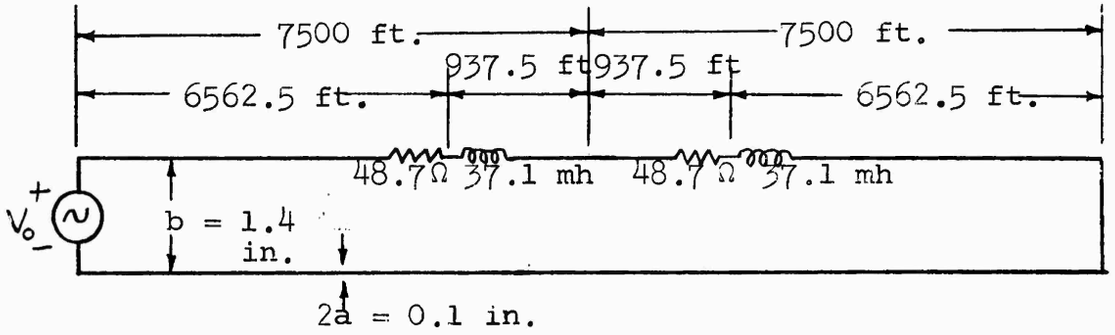

Figure 28. VLF side-loaded transmission-line antenna (Type II)

by arbitrarily letting Q = 100 at 21 kc. Impedance and efficiency characteristics of this antenna are shown in Figures 29 and 30. The zero reactance point occurs at 14.5 kc, where $R_{in} \approx 90\Omega$, $X_{in} \approx 0$, and efficiency = 6%.

As a final numerical example of a transmission-line antenna, we consider a Type III antenna. In a Type III antenna it is necessary that the side loads, Z_1 and Z_2, be different in order to obtain any appreciable antenna radiation. If $Z_1 = Z_2$, the structure is a symmetric, balanced transmission line which

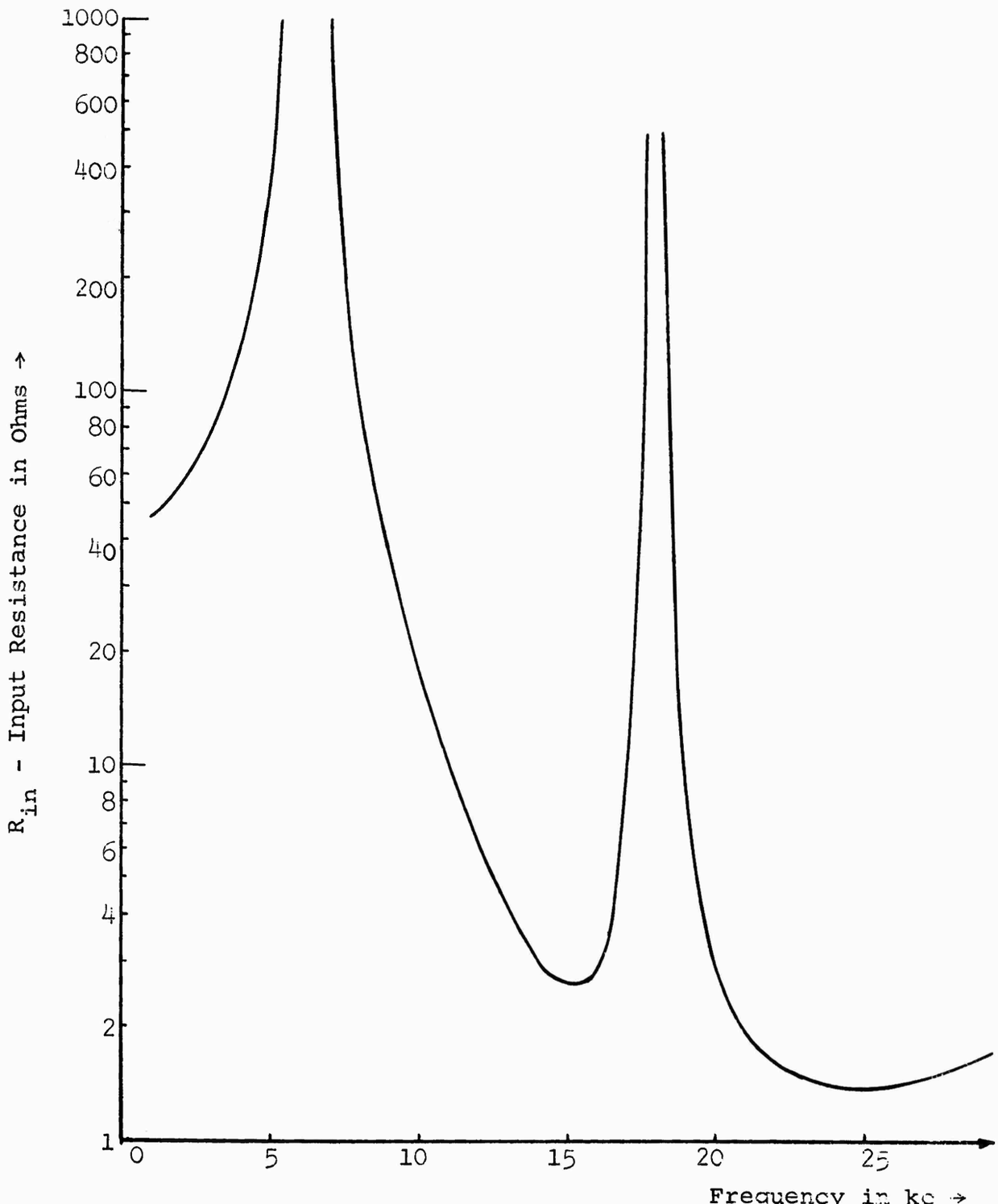

Figure 26. Theoretical input resistance of the Type I transmission-line antenna of Figure 25

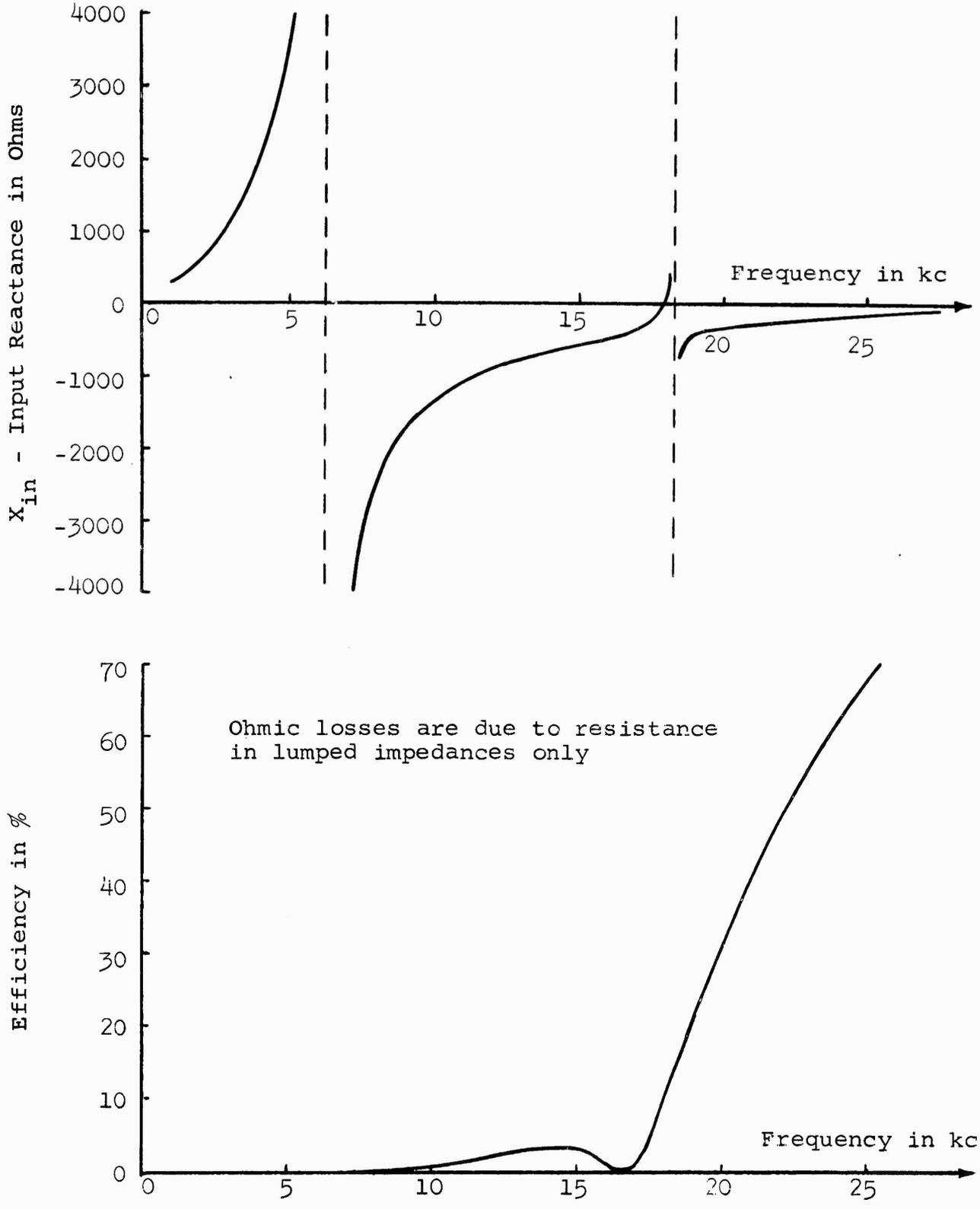

Figure 27. Theoretical input reactance and radiation efficiency of the Type I transmission-line antenna of Figure 25

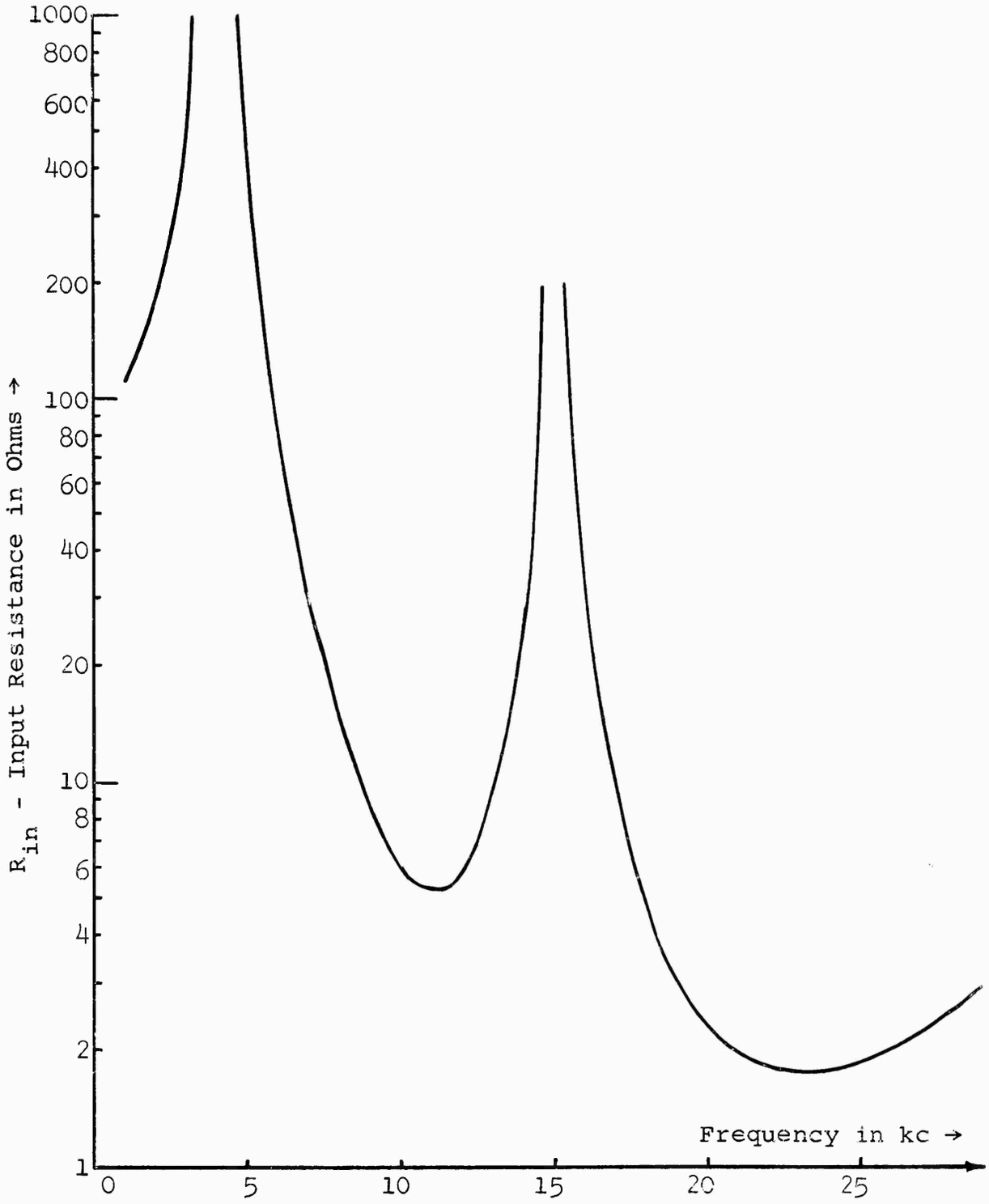

Figure 29. Theoretical input resistance of the Type II transmission-line antenna of Figure 28

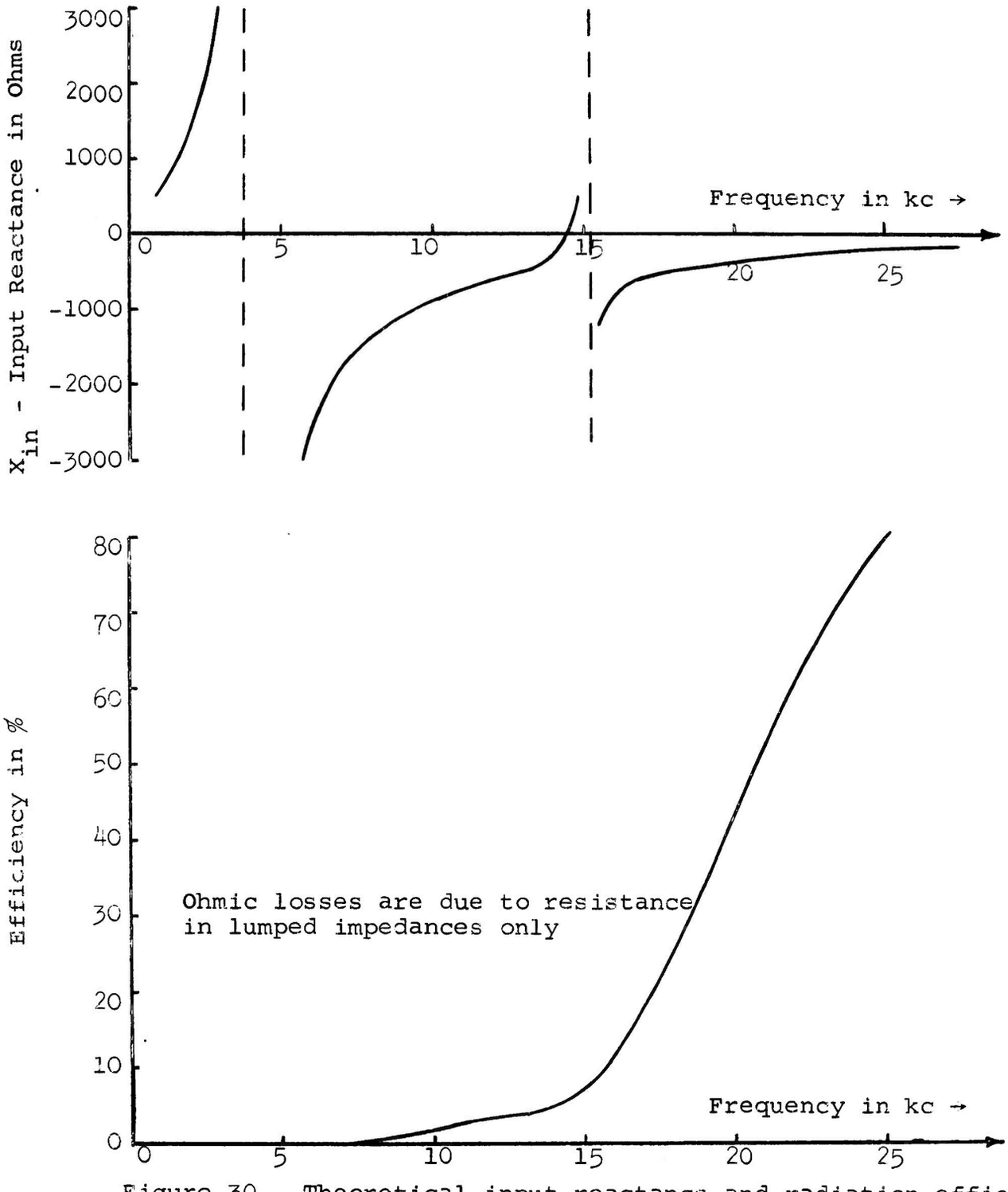

Figure 30. Theoretical input reactance and radiation efficiency of the Type II transmission-line antenna of Figure 28

produces a negligibly small radiation field. Equations for impedance and efficiency are given in [2, pp. 96-103]. The antenna is shown schematically in Figure 31, and the antenna characteristics are given in Figures 32 and 33. The resistances were

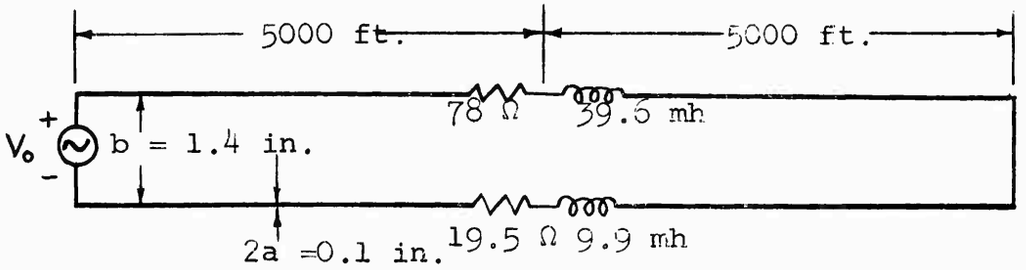

Figure 31. VLF side-loaded transmission-line antenna (Type III)

determined by letting Q = 100 at 31.3 kc. The zero reactance point occurs at 23.6 kc, where $R_{in} \approx 250\Omega$, $X_{in} \approx 0$, and efficiency = 41.5%.

It is important to note that the transmission-line antennas shown in Figures 22, 25, 28, and 31 are merely typical examples of VLF transmission-line antennas. By means of the proper adjustment of the size and spacing of the lumped impedances, many other combinations of impedance and efficiency can be realized for a given design frequency. The efficiency characteristics shown are based on the inductors having Q = 100 at some frequency; however if higher quality inductors are available, they may be used to achieve higher upper bounds on the efficiency.

In order to obtain a comparison of the radiation efficiency of trailing-wire and transmission-line antennas, efficiency characteristics of the 10,000-ft. and 15,000-ft. trailing wires and three types of transmission-line antennas (those of Figures

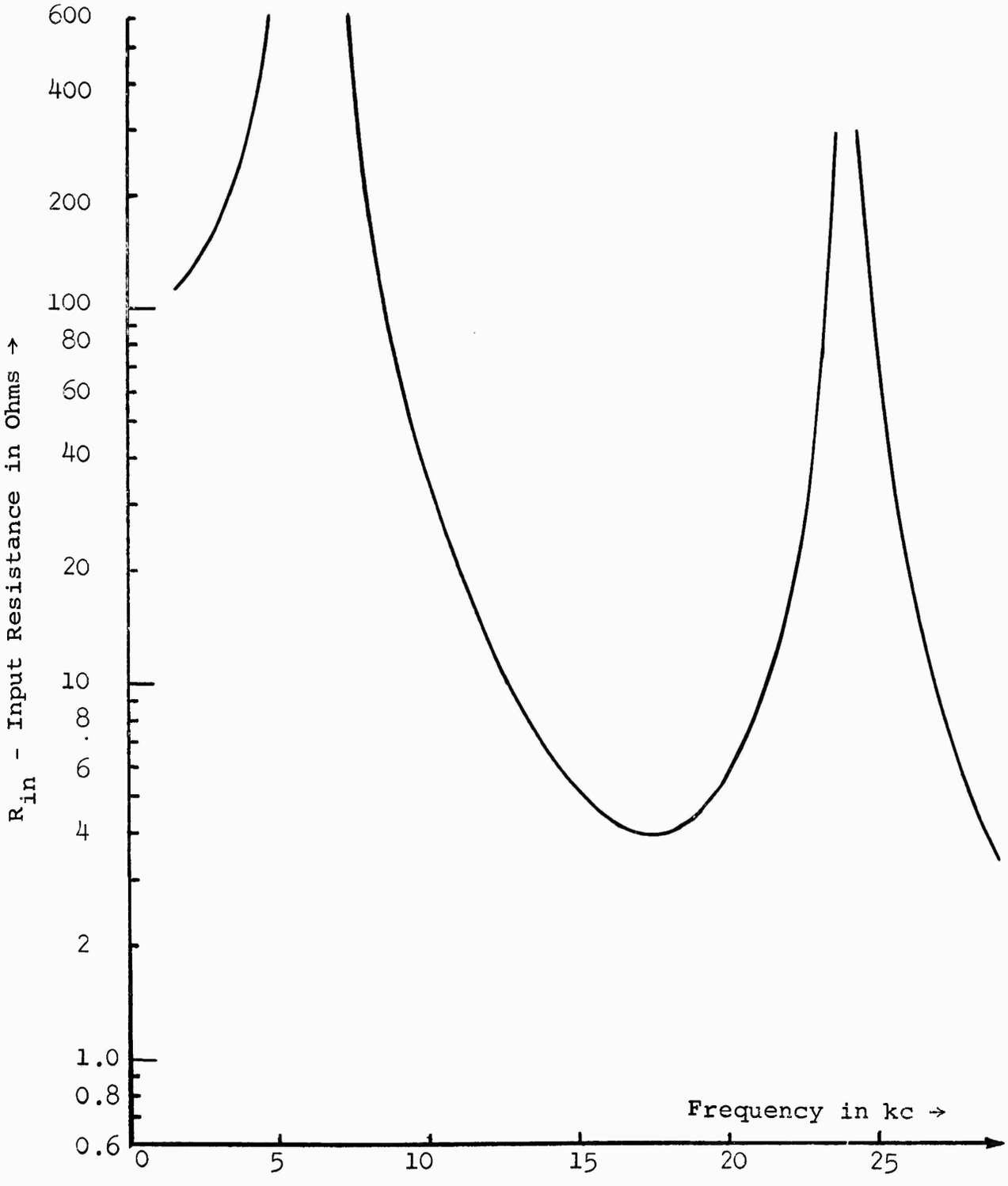

Figure 32. Theoretical input resistance of the Type III transmission-line antenna of Figure 31

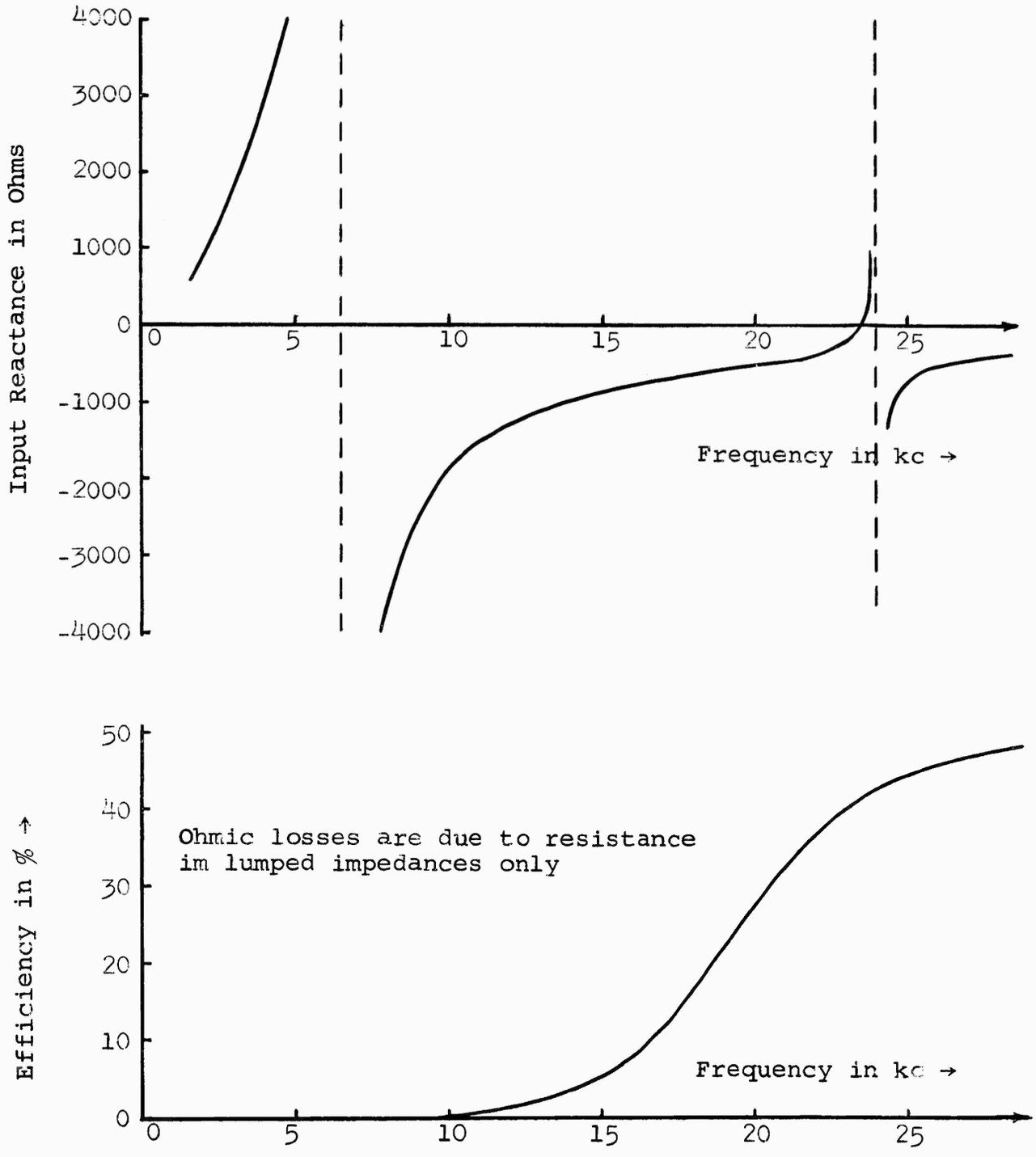

Figure 33. Theoretical input reactance and radiation efficiency of the Type III transmission-line antenna of Figure 31

25, 28, and 31) are shown in Figure 34. Any comparison derived from Figure 34 is biased in favor of the transmission-line antennas, since ohmic losses in the wires are not considered in the transmission-line antenna but are included in the trailing-wire antennas. In spite of this bias, it is obvious that the trailing-wire antennas are more efficient at the lower VLF frequencies (shorter electrical lengths). Even allowing for an appreciable loss of efficiency due to ohmic losses in the wires, the efficiency of Type I and II transmission-line antennas still appears comparable to that of the trailing-wire antennas for frequencies above 24 kc. However, Figures 26 and 29 show that for frequencies above 24 kc, the input resistance of the Type I and II antennas is very low. Such low input resistances would be difficult to match to a transmitter output impedance. This fact emphasizes the necessity of considering both efficiency and input impedance (not to mention mechanical and aerodynamic characteristics) when making a comparison of the two types of antennas.

It is necessary that the high-power airborne antennas under consideration be capable of operation at reasonably high altitudes in order to increase the communication range. Due to the increase in free ion density with increasing altitude, the problems of arc and corona discharges become more important, particularly for the high voltages which may be encountered with high-power antennas. Because of the close spacing of the wires

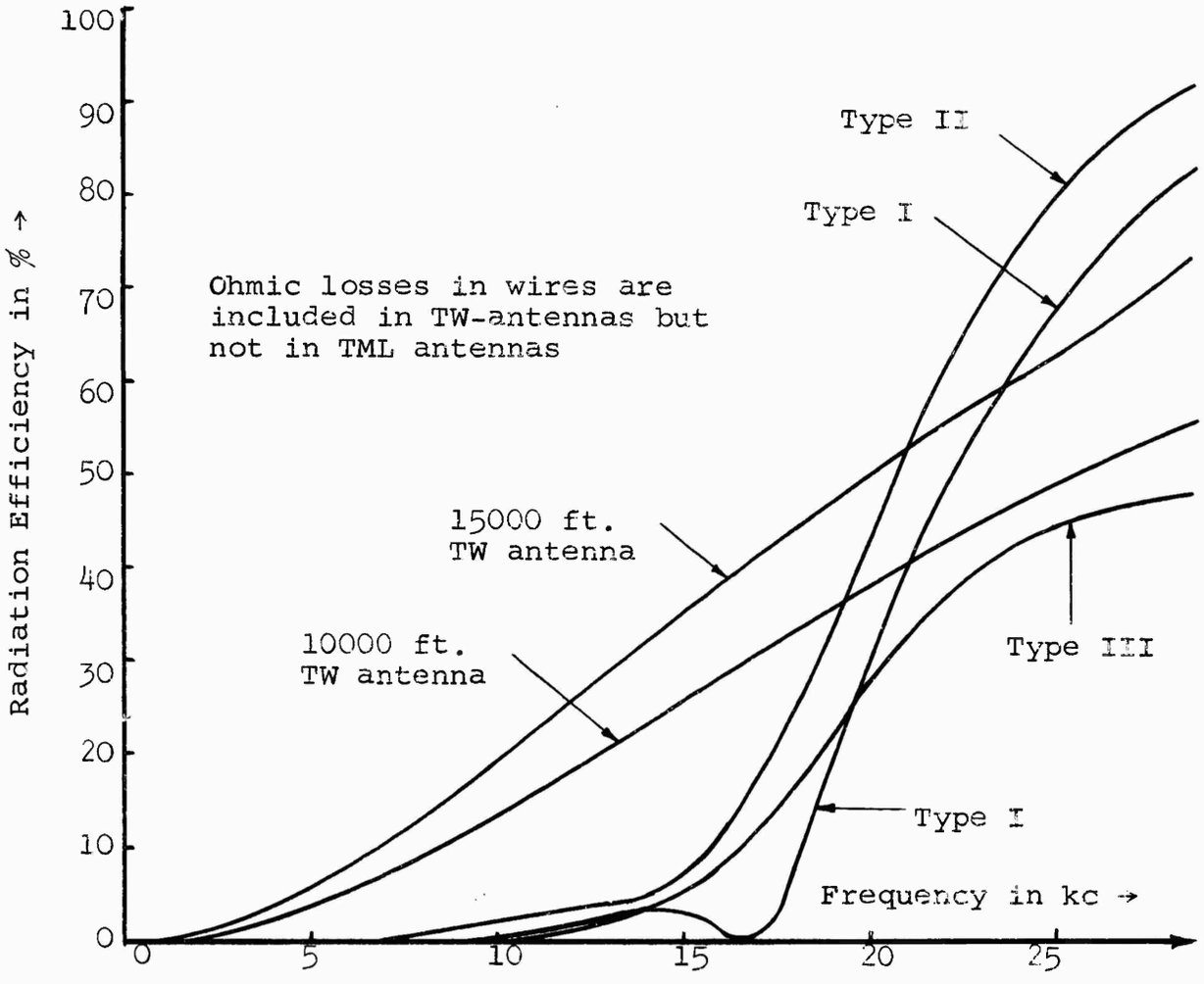

Figure 34. Comparison of the radiation efficiency of selected trailing-wire antennas and transmission-line antennas

in a transmission-line antenna and the presence of high-Q lumped impedances in the lines, it is expected that the transmission-line antenna will be susceptible to corona and arc discharges both across the line and through the lumped impedances. For the trailing-wire antenna, the largest potential gradient should occur at the point where the antenna is closest to the aircraft (i.e., the driving point). It is believed that by proper design and insulation of the terminal equipment, trailing-wire antennas can be operated at voltages up to 10 kilovolts peak at altitudes up to 35,000 feet.

Let us consider the magnitudes of the voltages across the lumped impedances of the antennas shown in Figures 25, 28, and 31. By straightforward algebraic manipulation of transmission-line antenna equations derived by Kulterman, expressions for the voltage drops across the lumped impedances of a transmission-line antenna can be derived.[2] These expressions are complex and will not be given here, since they would mean very little to the reader who is not familiar with reference [2]. An input voltage of one volt rms is assumed to be maintained across the input terminals as the frequency is varied over the VLF spectrum. The magnitudes of the voltages across the lumped impedances of the antennas of Figures 25, 28, and 31 are shown as a function of frequency in Figures 35, 36, and 37, respectively. It can be seen that over narrow frequency ranges within the VLF spectrum

[2] See [2] pp. 19-21 for Type I antennas, pp. 42-44 for Type II, and pp. 82-87 for Type III.

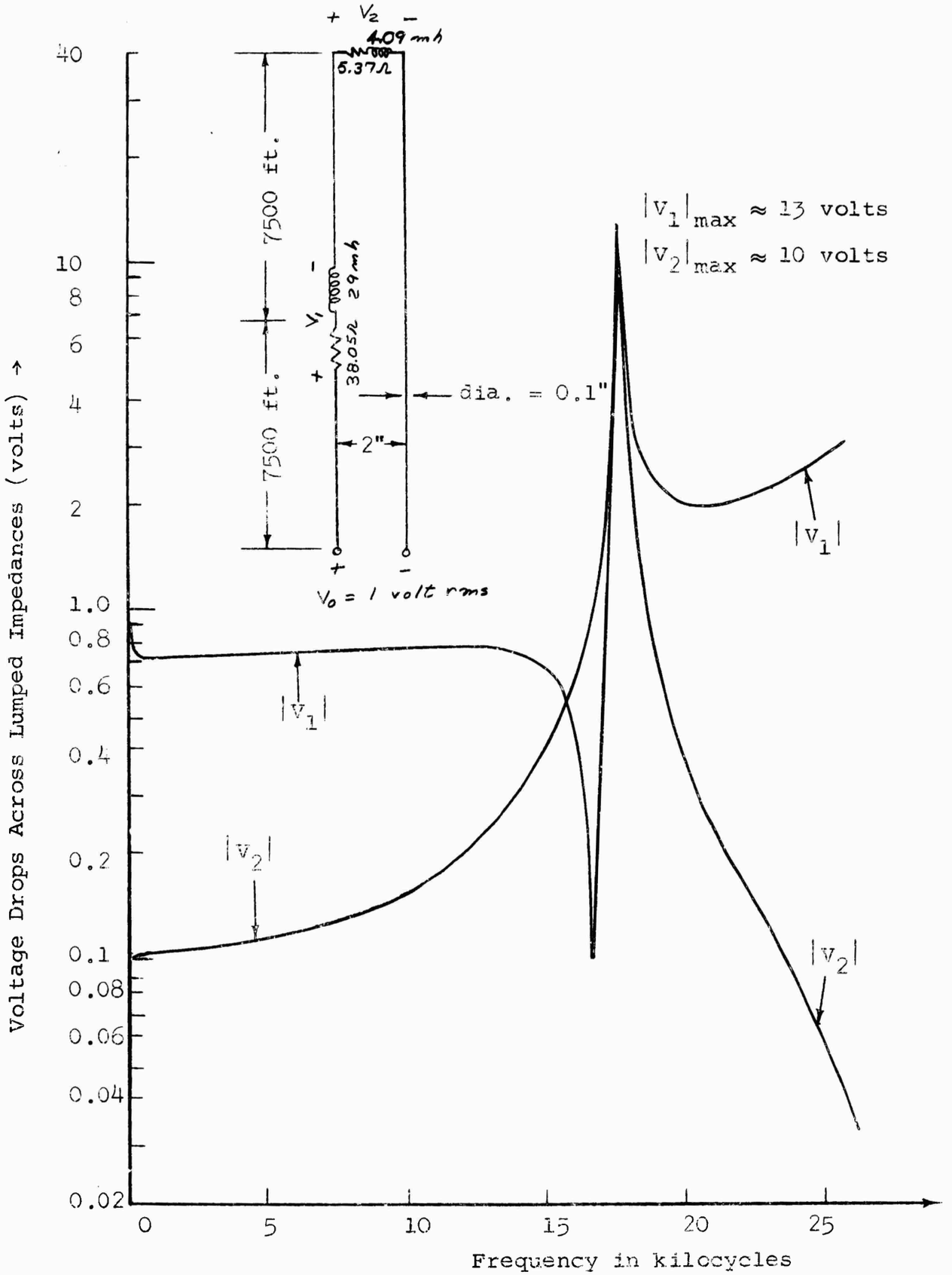

Figure 35. Side-load voltage drops for a Type I antenna

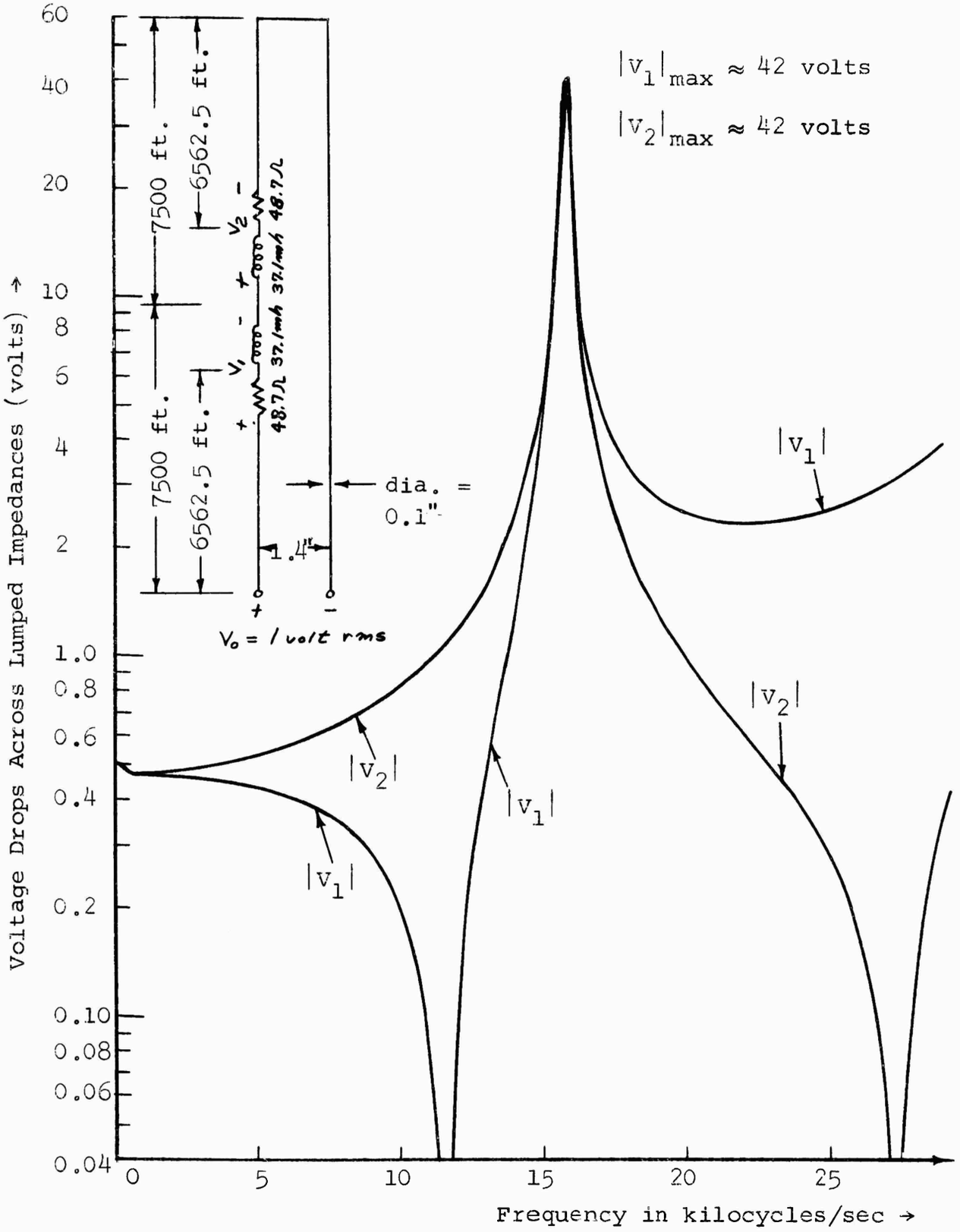

Figure 36. Side-load voltage drops for a Type II antenna

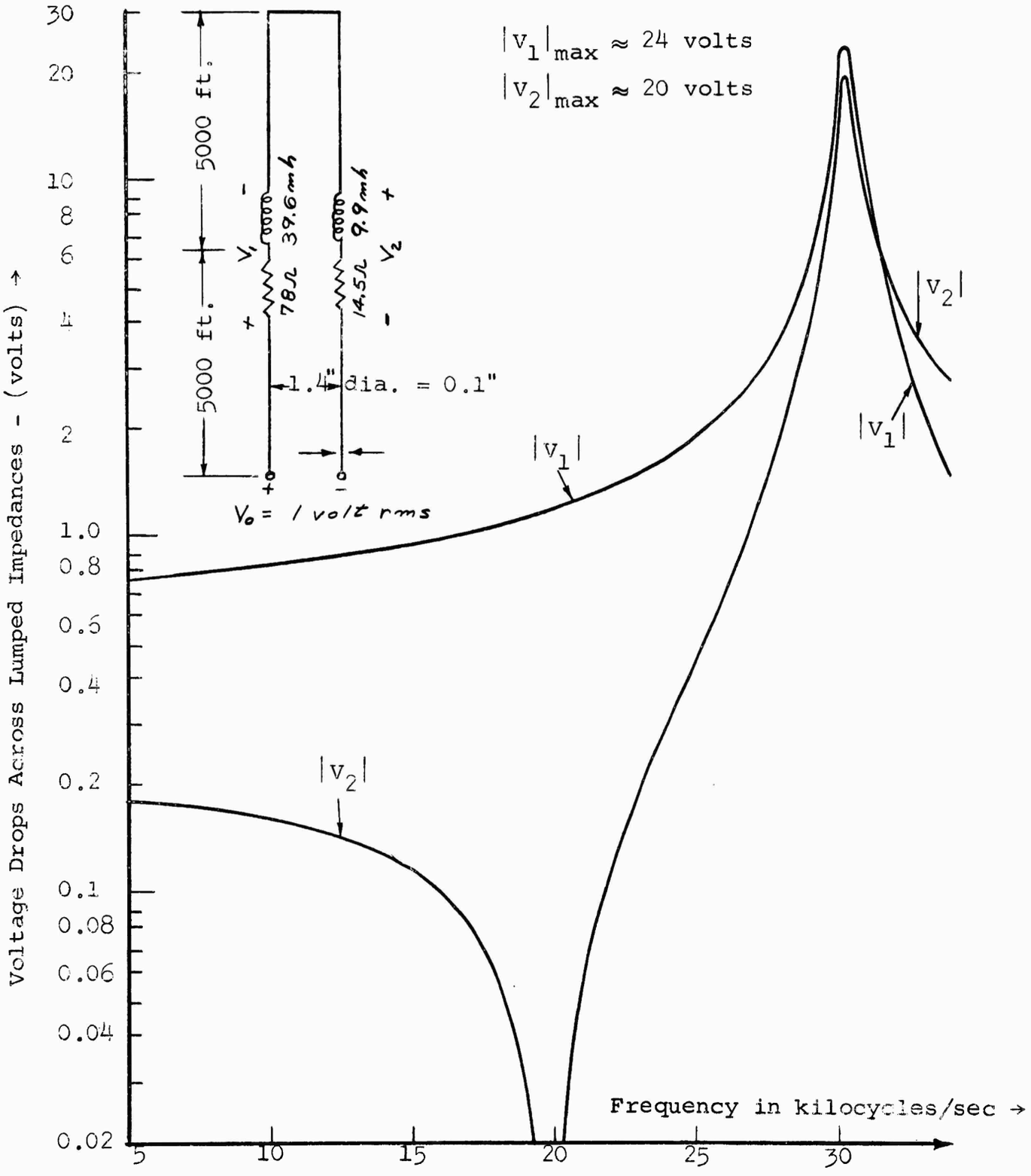

Figure 37. Side-load voltage drops for a Type III antenna

the maximum voltages across the high-Q impedances can range up to 10 to 42 volts rms for each volt rms at the input. For higher quality lumped impedances, the peak voltages can be still larger. In the practical case, the ohmic losses in the wires of the antenna will lower the Q of the circuit, so that the observed peak voltages should be lower than the theoretical values given. It should be noted that in the case of the Type I antenna, the voltage across the end load also appears across the line at that point. For the Type III antenna, the close proximity of the two lumped impedances increases the danger of arc formation. Thus, even allowing for a substantial lowering of the circuit Q by the ohmic losses in the wires, an appreciable multiplication of the input voltage can appear across the lumped impedances. A conflict in design criteria also arises for antennas operated near these critical frequencies, because low-Q impedances are required to minimize voltage breakdown, while high-Q impedances are required to maximize radiation efficiency.

5.0 CONCLUSIONS

Although one cannot state specifically which type of antenna is best for a given application without being given a complete set of design parameters and requirements, each type does possess some general advantages and disadvantages as listed below:

Trailing-Wire Antennas

Advantages:

1. Relatively good radiation efficiency for very short electrical lengths. They can be used at lower frequencies for a given length, or shorter lengths for a given frequency.
2. Very good radiation efficiency near $\ell/\lambda = 0.5$ (half-wave antiresonance).
3. Relatively simple mechanical construction and good aerodynamic characteristics compared with transmission-line antennas.
4. A given trailing-wire antenna is capable of being used at many frequencies and can be partially tuned in flight by extension or retraction of the wire.

Disadvantages:

1. Input reactance is strongly dependent on the aircraft and the input conditions, since the aircraft forms an active part of the radiating structure.

2. Input impedance characteristics are fixed for a given wire length, wire diameter, and aircraft. For some combination of aircraft capacitance and wire reactance it may be necessary to use an additional impedance matching network to match the antenna to the transmitter at the required frequency.

Transmission-Line Antennas

Advantages:

1. Offers virtually limitless capabilities of achieving desirable impedance characteristics for a given length of a line by adjusting the size and spacing of the lumped impedances.
2. Offers the possibility of relatively wide-band operation if the antenna operating frequency is located in the regions of slow variation of X_{in} and R_{in}.
3. Input impedance and radiation efficiency are virtually independent of the aircraft, since the aircraft forms only a small passive part of the radiating structure.
4. Antenna can be designed to furnish its own matching network for a given operating frequency.

Disadvantages:

1. Extremely low efficiency for very short electrical lengths. This is a result of the cancellation of almost equal and opposite currents in the two wires at the lower frequencies. Efficiency tends to be lower

than that of a trailing-wire antenna of the same length because the ohmic losses in the wires are roughly twice as large, and there are additional losses in the lumped impedances.

2. Complicated mechanical construction and poor aerodynamic characteristics (heavier, higher drag, more bulk, etc.) compared with trailing-wire antennas.
3. Susceptible to corona loss and voltage breakdown at high altitudes due to high voltage gradients at the lumped impedances.

REFERENCES

1. Buehler, W. E., and C. D. Lunden, "Impedance of Asymmetrically-Fed Trailing-Wire Antennas," Boeing Airplane Company, Document D6-8873, March 28, 1962.

2. Kulterman, R. W., "Linear Side-Loaded Transmission-Line Antennas," Technical Report EE-78, Engineering Experiment Station, University of New Mexico, Albuquerque, New Mexico, August, 1962.

3. King, R. W. P., The Theory of Linear Antennas, Harvard University Press, 1956, p. 192, p. 404.

4. Schelkunoff, S. A., Advanced Antenna Theory, John Wiley and Sons, Inc., New York, 1952, pp. 79-83.

5. _____, Applied Mathematics for Engineers and Scientists, D. Van Nostrand Company, Inc., New York, 1957, pp. 212-220.

6. Schelkunoff, S. A., and H. T. Friis, Antennas, Theory and Practice, John Wiley and Sons, Inc., New York, 1952, p. 431-432.

7. International Telephone and Telegraph Corp., Reference Data for Radio Engineers, Stratford Press, Inc., New York, 1956, p. 53.

8. King, R. W. P., H. R. Mimno, and A. H. Wing, Transmission Lines, Antennas, and Wave Guides, McGraw-Hill Book Co., Inc., 1945, pp. 113-114.

9. Kraus, J. D., Antennas, McGraw-Hill Book Co., Inc., New York, 1950, pp. 239-241.

10. Ramo, S., and J. R. Whinnery, Fields and Waves in Modern Radio, John Wiley and Sons, Inc., New York, 1953, pp. 349-350.

11. Dwight, H. B., Tables of Integrals and Other Mathematical Data, Macmillan Company, New York, 1957, pp. 276-277.

12. McLachlan, N. W., Bessel Functions for Engineers, Oxford University Press, London, 1934, pp. 182-183.

DISTRIBUTION LIST FOR UNCLASSIFIED REPORTS

CONTRACT Nonr 2798(01)(FBM)

Addressee	No. of Copies
Director Defense Documentation Center Cameron Station Alexandria, Virginia 22314	10
Chief of Naval Research Code 466 Code 427 Washington 25, D. C.	 3 1
Director, Special Projects (SP-204) Bureau of Naval Weapons Washington 25, D. C.	25
Commanding Officer Office of Naval Research, Branch Office 1030 East Green Street Pasadena 1, California	3
Chief of Naval Operations Op 07 Op 94T Washington 25, D. C.	 1 2
Chief, Bureau of Ships Navy Department Code 671C Code 679 Code 686 Code 687H Code 687A Washington 25, D. C.	 1 1 1 1 1
Director Naval Research Laboratory Code 5440 Code 5425 (Attn: Mr. L. S. Bearce) Code 5420 Code 5419 Code 5360 Code 5308 (Attn: Mr. John Barry) Code 2027 Washington 25, D. C.	 1 1 1 1 1 1 3

Addressee	No. of Copies
Commanding Officer and Director U. S. Navy Underwater Sound Laboratory Fort Trumbull New London, Conn. Attn: Mr. G. M. Milligan	1
Commanding Officer U. S. Naval Air Development Center Johnsville, Pa. Attn: Mr. E. Johnson, AEEL Mr. C. E. Keener, AWRD	1 1
Commanding Officer and Director U. S. Naval Ordnance Laboratory Corona, Calif. Attn: Mr. A. W. Walters Code 45	1
Commanding Officer and Director U. S. Naval Ordnance Laboratory White Oak, Maryland Attn: Mr. Robert J. Miller Code 042	1
Technical Director U. S. Naval Ordnance Test Station China Lake, Calif.	1
Commander U. S. Naval Ordnance Test Station 3202 East Foothill Blvd. Pasadena 8, California	1
Commanding Officer and Director U. S. Navy Underwater Sound Laboratory New London, Conn. Attn: Mr. C. B. Dunn	2
Commanding Officer and Director Naval Electronics Laboratory San Diego 52, California	1
Commanding Officer and Director U. S. Navy Mine Defense Laboratory Panama City, Florida Attn: Code 710	1
Mr. Martin G. Kraichman Naval Ordnance Laboratory White Oak, Maryland	1

Addressee	No. of Copies
Commanding General White Sands Missile Range New Mexico Attn: Technical Library RR-162	1
Program Director Advanced Science Programs National Science Foundation 1951 Constitution Ave. Washington 25, D. C.	1
National Science Foundation Engineering Program Washington 25, D. C.	1
National Research Council Committee on Undersea Warfare 2101 Constitution Ave., N.W. Washington 25, D. C.	1
Dr. J. R. Wait, Consultant Central Radio Propagation Laboratory National Bureau of Standards Boulder, Colorado	2
Mr. Kenneth A. Norton, Chief Radio Propagation Engineering Division Central Radio Propagation Laboratory National Bureau of Standards Boulder, Colorado	1
Dr. Cullen Crain Rand Corporation Santa Monica, California	1
Director Woods Hole Oceanographic Institution Woods Hole, Mass. Attn: Dr. Hersey	1
Director Scripps Institution of Oceanography La Jolla, Calif.	1
Mr. J. Y. Wong Antenna Group (Microwave Section) National Research Council of Canada Ottawa 2, Ontario, Canada	1
Stanford Electronics Laboratories Stanford University Stanford, California	1

Addressee	No. of Copies
Stanford Research Institute Menlo Park, California Attn: Mr. Geo. H. Hagn	1
Mr. L. H. Rorden Stanford Research Institute Menlo Park, California	1
Applied Physics Laboratory Johns Hopkins University Attn: Comdr. Pollow 8621 Georgia Avenue Silver Spring, Maryland	1
Dr. L. Katz Applied Physics Laboratory Johns Hopkins University Silver Spring, Maryland	1
Director Research Laboratory of Electronics Mass. Institute of Technology Cambridge 39, Mass.	1
Dr. R. W. P. King Cruft Laboratory Harvard University Cambridge 38, Mass.	1
Electrical Engineering Research Document File School of Electrical Engineering Cornell University Ithaca, New York	1
University of Chicago Laboratories for Applied Science Museum of Science Chicago 37, Ill. Attn: Mr. Van Zeelind	1
Director, Hudson Laboratories Columbia University P. O. Box 329 Dobbs Ferry, New York	1
Dr. J. H. Milligan, Jr. Chairman, Elec. Engr. Dept. New York University New York 53, N. Y.	1

Addressee	No. of Copies
Dr. B. M. Fannin Electrical Engineering Research Laboratory University of Texas Austin 3, Texas	1
Ordnance Research Laboratory Pennsylvania State University P. O. Box 30 University Park, Pa.	1
Dr. R. H. Duncan Physical Science Laboratory New Mexico State University University Park Las Cruces, New Mexico	1
University of New Mexico EE Dept.	1
Dr. R. K. Moore Center for Research in Engineering Science University of Kansas Rural Route #4 Lawrence, Kansas	1
Mr. Albert R. Giddis Project Engineer Advance Programs Section Philco Corporation Western Development Laboratory 3875 Fabian Way Palo Alto, California	1
Dr. Ronald V. Row Sylvania Electronic Systems Division of Sylvania Electric Products, Inc. 100 First Ave. Waltham 54, Massachusetts	1
Development Engineering Company Boulder, Colorado Attn: Mr. Don Watt	1
Development Engineering Company Leesburg, Virginia Attn: Mr. Lucien Rawls	1
Space Electronics Corporation 1200 AirWay Glendale 1, California Attn: Mr. Frank W. Lehan	1

Addressee	No. of Copies
Mr. Harold A. Wheeler Wheeler Laboratories, Inc. 122 Cutter Mill Road Great Neck, N. Y.	1
Stromberg-Carlson Division of General Dynamics Rochester, N. Y. Attn: Victor Savchuk	1
Mr. Martin Katzin Electromagnetic Research Corp. 5001 College Avenue College Park, Maryland	1
Research Division Electronics Communications, Inc. 1830 York Road Timonium, Maryland Attn: Technical Library	1
Mr. Richard C. Becker Senior Staff Engineer Amphenol-Borg Electronics Corp. 25th Ave. at Cermak Broadview, Ill.	1